

Cite this: DOI: 10.1039/c7dt03362a

# *ortho*-Cycloalkyl substituted *N,N'*-diaryliminoacenaphthene-Ni(II) catalysts for polyethylene elastomers; exploring ring size and temperature effects†

Hongyi Suo,<sup>a,b</sup> Irina V. Oleynik,<sup>c</sup> Chuanbing Huang,<sup>a,b</sup> Ivan I. Oleynik,<sup>\*c</sup> Gregory A. Solan,<sup>†\*a,d</sup> Yanping Ma,<sup>†a</sup> Tongling Liang<sup>†a</sup> and Wen-Hua Sun<sup>†\*a,b</sup>

A family of six unsymmetrical *N,N'*-diiminoacenaphthene-nickel(II) bromide complexes, [1-(2,6-(Ph<sub>2</sub>CH)<sub>2</sub>-4-MeC<sub>6</sub>H<sub>2</sub>N)-2-(ArN)<sub>2</sub>C<sub>10</sub>H<sub>6</sub>]NiBr<sub>2</sub> (Ar = 2-(C<sub>6</sub>H<sub>11</sub>)-6-MeC<sub>6</sub>H<sub>2</sub> **Ni1**, 2-(C<sub>5</sub>H<sub>9</sub>)-6-MeC<sub>6</sub>H<sub>2</sub> **Ni2**, 2-(C<sub>8</sub>H<sub>15</sub>)-6-MeC<sub>6</sub>H<sub>2</sub> **Ni3**, 2-(C<sub>6</sub>H<sub>11</sub>)-4,6-Me<sub>2</sub>C<sub>6</sub>H<sub>2</sub> **Ni4**, 2-(C<sub>5</sub>H<sub>9</sub>)-4,6-Me<sub>2</sub>C<sub>6</sub>H<sub>2</sub> **Ni5**, 2-(C<sub>8</sub>H<sub>15</sub>)-4,6-Me<sub>2</sub>C<sub>6</sub>H<sub>2</sub> **Ni6**), each bearing one ring-size variable 4-R-2-methyl-6-cycloalkyl-substituted *N*-aryl group and one *N'*-4-methyl-2,6-dibenzhydrylphenyl group, have been prepared and fully characterized. The molecular structures of **Ni1**, **Ni2**, **Ni3** and **Ni5** reveal distorted tetrahedral geometries with different degrees of steric protection imparted by the two inequivalent *N*-aryl groups. On activation with either EASC or MMAO, all the precatalysts are highly active (up to 17.45 × 10<sup>6</sup> g PE mol<sup>-1</sup> (Ni) h<sup>-1</sup>) for ethylene polymerization at 20–50 °C with their activities correlating with the type of cycloalkyl *ortho*-substituent: cyclooctyl (**Ni6**, **Ni3**) > the cyclopentyl (**Ni5**, **Ni2**) > cyclohexyl (**Ni4**, **Ni1**) for either R = H or Me. Moderately branched polyethylenes (*T<sub>m</sub>*'s as low as 44.2 °C) can be obtained with molecular weights in the range 2.14–6.68 × 10<sup>5</sup> g mol<sup>-1</sup> with the branching content enhanced by the temperature of the polymerization. Dynamic mechanical analysis (DMA) and monotonic tensile stress–strain tests have been employed on the polyethylene samples and reveal the more branched materials to show good elastic recovery properties (up to 75.5%).

Received 10th September 2017,  
Accepted 16th October 2017

DOI: 10.1039/c7dt03362a

rsc.li/dalton

## Introduction

Since the first reports of  $\alpha$ -diimine-M (M = Ni, Pd) catalysts for the polymerization of ethylene in the mid-1990s,<sup>1</sup> the important role played by steric properties in the suppression of chain termination processes has been recognized.<sup>2</sup> In particular, the strategic positioning of alkyl substituents (*e.g.*, methyl, isopropyl *etc.*) at the *ortho*-positions of the *N*-aryl groups of the catalyst and the resulting axial protection of the active species

has facilitated the formation of linear to branched polyethylenes (see **A**, Chart 1).

With the advances in *ortho*-substituted aniline synthesis, more sterically demanding  $\alpha$ -diimine derivatives have been reported which in-turn have allowed for catalysts that are not only more active, but are also more thermally robust and yield polymers with a range of molecular weights and branching contents.<sup>3,4</sup> For example, the incorporation of benzhydryl groups as the *ortho*-substituents (**B**, Chart 1),<sup>5</sup> has led to

<sup>a</sup>Key Laboratory of Engineering Plastics and Beijing National Laboratory for Molecular Sciences, Institute of Chemistry, Chinese Academy of Sciences, Beijing 100190, China. E-mail: whsun@iccas.ac.cn

<sup>b</sup>CAS Research/Education Center for Excellence in Molecular Sciences, University of Chinese Academy of Sciences, Beijing 100049, China

<sup>c</sup>N.N. Vorozhtsov Novosibirsk Institute of Organic Chemistry, Pr. Lavrentjeva 9, Novosibirsk 630090, Russia. E-mail: oleynik@nioch.nsc.ru

<sup>d</sup>Department of Chemistry, University of Leicester, University Road, Leicester LE1 7RH, UK. E-mail: gas8@leicester.ac.uk

† Electronic supplementary information (ESI) available. CCDC 1573415–1573418 for **Ni1**, **Ni2**, **Ni3** and **Ni5**. For ESI and crystallographic data in CIF or other electronic format see DOI: 10.1039/c7dt03362a

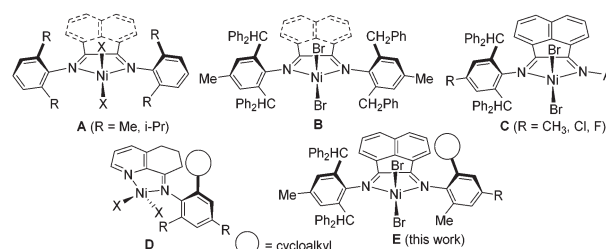


Chart 1 Development of  $\alpha$ -diiminonickel(II) halide precatalysts.

reports of catalysts that display high productivity and operate with remarkable thermostability (90 °C or higher), a feature that has been attributed to the slowing down of chain transfer processes as well as inhibition of deactivation pathways.<sup>3a,4c,f,6</sup> More recently, nickel catalysts bearing unsymmetrical  $\alpha$ -diimines have been disclosed which benefit from the steric properties of a *N*-4-*R*-2,6-dibenzhydrylphenyl group and the tunability of a less sterically bulky *N*-aryl group (C, Chart 1).<sup>7</sup> Interestingly, these types of catalysts also combine highly activity with high thermal stability and what is more allow access to highly branched polyethylenes. Elsewhere, cycloalkyl groups have started to emerge as compatible *ortho*-substituents with nickel-based polymerization precatalysts such as **D** reported (Chart 1).<sup>8</sup> Notably, this class of nickel catalyst display high activity and produce polyethylenes with unusual branching architectures that exhibit low molecular weights and narrow polydispersity.

In recent years our group has been interested in designing new  $\alpha$ -diimine-nickel catalysts that are capable of mediating the formation of hyperbranched polyethylenes that could potentially be used as thermoplastic elastomers (TPEs). Such materials are attracting widespread interest in academia and industry owing to their growing demand in applications such as the automotive, gaskets, footwear, industrial hose and clothing industries.<sup>9</sup> However, due to the complexity of some of the current synthetic approaches,<sup>10,11</sup> we have been drawn to the simplicity of a homo-polymerization of ethylene as a more straightforward approach to TPEs and indeed have had some success in this endeavour using precatalysts of type C (Chart 1).<sup>12</sup>

Herein we target a new family of unsymmetrical *N,N'*-diiminoacenaphthene-nickel(II) bromide complexes (**E**, Chart 1), incorporating one sterically demanding 4-methyl-2,6-dibenzhydrylphenyl *N*-aryl group while the other, 4-*R*-2-methyl-6-cycloalkylphenyl, contains a cycloalkyl *ortho*-substituent that can be systematically modified in terms of ring size (*viz.*, cyclopentyl *vs.* cyclohexyl *vs.* cyclooctyl). In addition, the 4-*R* group presents a further site that will be probed with a view to exploring possible inductive effects. An in-depth study will then be initiated to optimize catalytic performance and to examine how these structural features impact on catalytic activity and the branching content of the resulting polyethylenes. A study of the mechanical properties of selected polymer samples will then be conducted to assess their elastomeric properties.

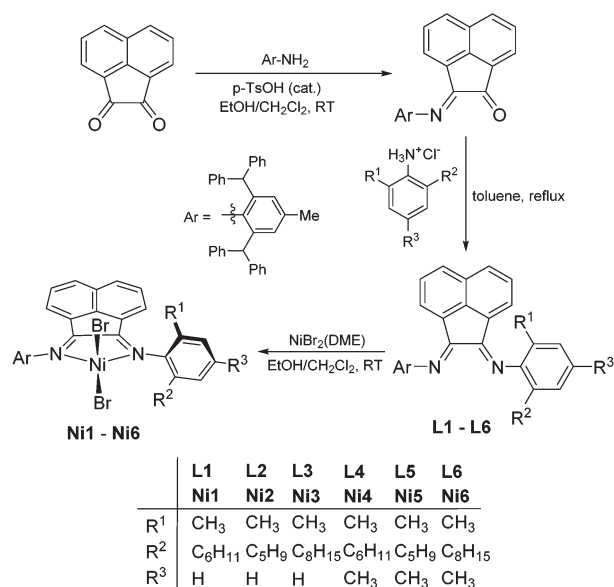
## Results and discussion

### Synthesis and characterization

The *N,N'*-diiminoacenaphthene-nickel(II) bromides, [1-{2,6-(Ph<sub>2</sub>CH)<sub>2</sub>-4-MeC<sub>6</sub>H<sub>2</sub>N}-2-(ArN)C<sub>2</sub>C<sub>10</sub>H<sub>6</sub>}]NiBr<sub>2</sub> (Ar = 2-(C<sub>6</sub>H<sub>11</sub>)-6-MeC<sub>6</sub>H<sub>2</sub> **Ni1**, 2-(C<sub>5</sub>H<sub>9</sub>)-6-MeC<sub>6</sub>H<sub>2</sub> **Ni2**, 2-(C<sub>8</sub>H<sub>15</sub>)-6-MeC<sub>6</sub>H<sub>2</sub> **Ni3**, 2-(C<sub>6</sub>H<sub>11</sub>)-4,6-Me<sub>2</sub>C<sub>6</sub>H<sub>2</sub> **Ni4**, 2-(C<sub>5</sub>H<sub>9</sub>)-4,6-Me<sub>2</sub>C<sub>6</sub>H<sub>2</sub> **Ni5**, 2-(C<sub>8</sub>H<sub>15</sub>)-4,6-Me<sub>2</sub>C<sub>6</sub>H<sub>2</sub> **Ni6**), can be readily prepared in reasonable to good yield by treatment of the corresponding ligand, **L1–L6**, with NiBr<sub>2</sub>(DME) (DME = 1,2-dimethoxyethane) in a

mixture of dichloromethane and ethanol at ambient temperature (Scheme 1). The ligands are novel and can be synthesized in a two step procedure involving firstly condensation of acenaphthylene-1,2-dione with one equivalent of 2,6-benzhydryl-4-methylaniline<sup>7a,c</sup> to form imine-ketone, 2-(2,6-dibenzhydryl-4-methylphenylimino)acenaphthyleneone, which can then be further condensed with the corresponding aniline hydrochloride<sup>8g</sup> to form **L1–L6** in modest yields. All the ligands have been characterized by FT-IR, <sup>1</sup>H/<sup>13</sup>C NMR spectroscopy and elemental analysis. The complexes have been similarly characterized and in addition for **Ni1**, **Ni2**, **Ni3** and **Ni5** by single crystal X-ray diffraction.

Single crystals of **Ni1**, **Ni2**, **Ni3** and **Ni5** suitable for the X-ray determinations were grown by slow diffusion of hexane into a dichloromethane solution of the corresponding complex. Perspective views of **Ni1**, **Ni2**, **Ni3** and **Ni5** are shown in Fig. 1–4; selected bond lengths and angles are listed in Table 1. The structures are closely related and will be discussed together. **Ni1**, **Ni2**, **Ni3** and **Ni5** all consist of a single nickel center surrounded by two nitrogen atoms belonging to a bidentate *N,N'*-diiminoacenaphthene and two bromide ligands to complete a geometry best described a distorted tetrahedral; similar structural features have been reported for a variety of unsymmetrical 1,2-diiminoacenaphthene derivatives.<sup>7a</sup> The key difference between the structures in this study relates to the nature of aryl group linked to imine-N2; in **Ni1** it is a 2-cyclohexyl-6-methylphenyl, in **Ni2** 2-cyclopentyl-6-methylphenyl, in **Ni3** 2-cyclooctyl-4,6-dimethylphenyl and **Ni5** 2-cyclopentyl-4,6-dimethylphenyl. With regard to the cycloalkyl *ortho*-substituent, a boat-chair conformation is adopted by the cyclooctyl ring (**Ni3**), a chair conformation for cyclohexyl (**Ni1**) and an envelope conformation for the cyclopentyl unit (**Ni5**, **Ni2**).<sup>13</sup> For all four structures the second imine-nitrogen (N1) is linked to the same sterically bulky 4-methyl-2,6-dibenz-



Scheme 1 Synthesis of **L1–L6** and **Ni1–Ni6**.

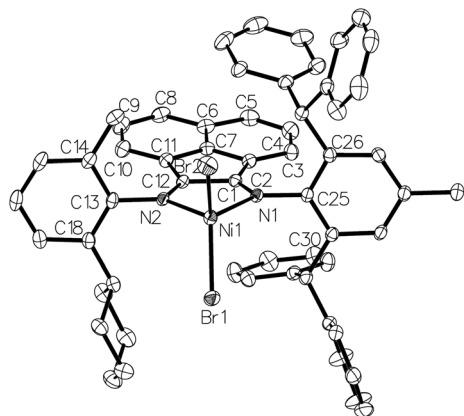


**Fig. 1** OLEX2 representation of Ni1 with the thermal ellipsoids shown at the 30% probability level; all hydrogen atoms have been omitted for clarity.

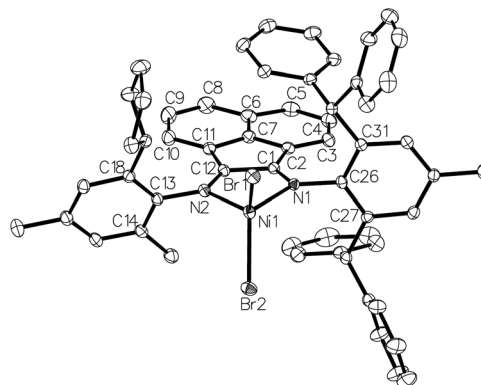


**Fig. 4** OLEX2 representation of Ni4 with the thermal ellipsoids shown at the 30% probability level; all hydrogen atoms have been omitted for clarity.

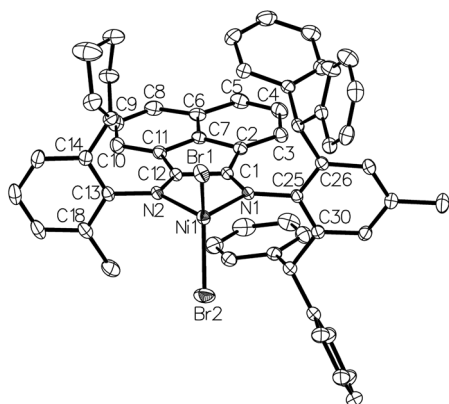


**Fig. 2** OLEX2 representation of Ni2 with the thermal ellipsoids shown at the 30% probability level; all hydrogen atoms have been omitted for clarity.

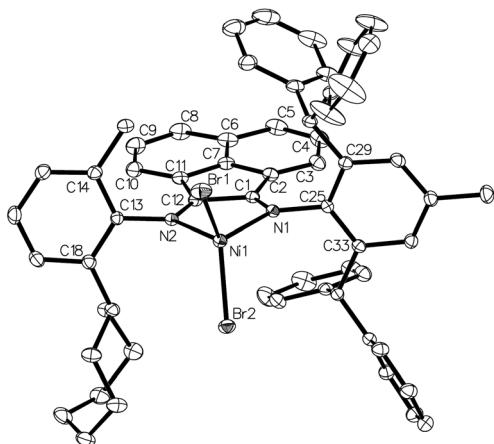


**Fig. 3** OLEX2 representation of Ni3 with the thermal ellipsoids shown at the 30% probability level; all hydrogen atoms have been omitted for clarity.

**Table 1** Selected bond lengths (Å) and angles (°) for Ni1, Ni2, Ni3 and Ni5

	Ni1	Ni2	Ni3	Ni5
Bond lengths (Å)				
Ni(1)–Br(1)	2.3378(6)	2.3294(9)	2.3481(8)	2.3274(6)
Ni(1)–Br(2)	2.3277(6)	2.3436(8)	2.3333(7)	2.3428(7)
Ni(1)–N(1)	2.035(2)	2.040(3)	2.036(2)	2.029(2)
Ni(1)–N(2)	2.024(2)	2.020(3)	2.023(2)	2.036(3)
N(1)–C(1)	1.289(3)	1.289(5)	1.283(3)	1.292(4)
N(1)–C(25)	1.449(3)	1.448(5)	1.452(3)	1.446(4)
N(2)–C(12)	1.284(3)	1.288(5)	1.283(3)	1.281(4)
N(2)–C(23)	1.449(3)	1.445(5)	1.443(3)	1.449(4)
Bond angles (°)				
N(1)–Ni(1)–N(2)	82.87(8)	82.86(14)	82.61(8)	83.26(10)
Br(1)–Ni(1)–Br(2)	122.84(2)	125.31(3)	122.28(2)	124.39(3)
N(1)–Ni(1)–Br(1)	111.17(6)	109.33(10)	114.50(6)	110.47(7)
N(2)–Ni(1)–Br(1)	110.10(6)	110.76(10)	106.52(6)	119.14(8)
N(1)–Ni(1)–Br(2)	112.14(6)	112.34(10)	111.89(6)	109.11(7)
N(2)–Ni(1)–Br(2)	110.62(6)	108.11(10)	111.75(6)	102.79(8)

hydrolyphenyl group. The bite angles for the bidentate ligands are similar [N1–Ni1–N2: 82.78(8) (Ni1), 82.86(14) (Ni2), 82.61(8) (Ni3), 83.26(10)° (Ni5)], while the Br1–Ni–Br2 angles show some modest variation (range: 122.28(2)–125.31(3)°). Despite the inequivalent steric and electronic properties of the cycloalkyl-substituted *N*-aryl groups, there are only minor differences in the corresponding Ni1–N2 bond distances (range: 2.020(3)–2.036(3) Å). The N1–C1 [1.289(3) Å (Ni1), 1.289(5) Å (Ni2), 1.283(3) Å (Ni3), 1.292(4) Å (Ni5)] and N2–C12 [1.284(3) Å (Ni1), 1.288(5) Å (Ni2), 1.283(3) Å (Ni3), 1.281(4) Å (Ni5)] bond lengths are consistent with C=N double bond character, while the imine vectors are essentially co-planar with the neighboring acenaphthene unit. In all cases the 4-methyl-2,6-dibenzhydryl phenyl group adopts an orientation almost perpendicular to the corresponding N1, N2, Ni1 plane (range: 85.11–88.38°). By contrast, the cycloalkyl-substituted *N*-aryl group shows some variation in the degree of inclination [88.47° (Ni1), 87.46° (Ni2), 76.73° (Ni3), 72.61° (Ni5)]. The bulky cyclooctyl group in Ni3 is likely responsible for the observed tilting of the aryl group away from perpendicular,

however, it is unclear why the *ortho*-cyclopentyl groups in **Ni2** in **Ni5** show such a difference in inclination.

Both the ligands, **L1–L6**, and complexes, **Ni1–Ni6**, exhibit two imine absorption bands in their IR spectra with the pair for the complexes shifted to lower wavenumber by *ca.* 20 cm<sup>-1</sup>, an observation that is consistent with effective coordination between the metal and the two imine nitrogen atoms. All the complexes display microanalytical data that is in accord with their elemental composition.

### Catalyst evaluation for ethylene polymerization

**Co-catalyst screen.** With the aim to identify the most suitable co-catalyst for the polymerization, **Ni6** was chosen as the test precatalyst and the type of aluminum alkyl co-catalyst varied with the pressure of ethylene maintained at 10 atmospheres and the run temperature at 30 °C (Table 2). In particular, four co-catalysts were evaluated namely methylaluminumoxane (MAO), modified methylaluminumoxane (MMAO), ethylaluminum sesquichloride (EASC) and diethylaluminum chloride (Et<sub>2</sub>AlCl). In each case very high activities for ethylene

polymerization were observed with the order, in terms of co-catalyst, following: EASC > Et<sub>2</sub>AlCl > MMAO > MAO. While it is clear that all the co-catalysts employed are effective at activating **Ni6**,<sup>14</sup> it is unclear why the chloroaluminum-type co-catalysts deliver higher activities [13.79–16.23 × 10<sup>6</sup> g PE mol<sup>-1</sup> (Ni) h<sup>-1</sup>] than their aluminumoxane counterparts [10.84–10.93 × 10<sup>6</sup> g PE mol<sup>-1</sup> (Ni) h<sup>-1</sup>]. Nevertheless, similar observations have been noted elsewhere for related nickel precatalysts.<sup>3b,15</sup> Based on catalytic activity, EASC and MMAO were selected as representative members of each type of activator for subsequent evaluations.

**Optimization and evaluation of Ni1–Ni6/EASC.** With a view to optimizing the reaction conditions and exploring the effect of these conditions on the polymer structure, **Ni6** was again used as the test precatalyst, this time using solely EASC as the co-catalyst. In particular, a study was conducted to determine the optimal molar ratio of Al to Ni, temperature and run time; the results are collected in Table 3.

Firstly, on increasing the molar ratio of Al/Ni from 400 to 900, with the temperature kept at 30 °C and the duration of the run at 30 minutes, the activity increased to a very high level of 17.45 × 10<sup>6</sup> g PE mol<sup>-1</sup> (Ni) h<sup>-1</sup> with an Al/Ni ratio of 700 (entries 1–6, Table 3), which is much higher than that observed with precatalysts of similar structure reported elsewhere.<sup>7a</sup> Notably as the number of molar equivalents of EASC is increased from 400 to 900 the molecular weight steadily drops. This observation is consistent with previous findings,<sup>7c,16</sup> and can be attributed to increased chain transfer from the active nickel species to aluminum yielding polyethylenes with lower molecular weight and narrower molecular weight distribution (see Fig. 5a).

Secondly, to understand the influence of reaction temperature, the polymerization was studied at temperatures between

**Table 2** Ethylene polymerization using **Ni6** with four different co-catalysts<sup>a</sup>

Entry	Co-cat.	Al/Ni	Yield (g)	Activity <sup>b</sup>	<i>M<sub>w</sub></i> <sup>c</sup>	<i>M<sub>w</sub></i> / <i>M<sub>n</sub></i> <sup>c</sup>	<i>T<sub>m</sub></i> <sup>d</sup> (°C)
1	MAO	2000	10.84	10.84	4.27	2.62	57.5
2	MMAO	2000	10.93	10.93	4.45	2.48	66.5
3	EASC	500	16.23	16.23	3.89	2.25	44.4
4	Et <sub>2</sub> AlCl	500	13.78	13.78	3.94	2.29	49.1

<sup>a</sup> Conditions: 2.0 μmol of **Ni6**; 10 atm of ethylene; total volume 100 mL; 30 min; 30 °C. <sup>b</sup> Activity: 10<sup>6</sup> g PE mol<sup>-1</sup> (Ni) h<sup>-1</sup>. <sup>c</sup> *M<sub>w</sub>*: 10<sup>5</sup> g mol<sup>-1</sup>; *M<sub>w</sub>* and *M<sub>w</sub>*/*M<sub>n</sub>* determined by GPC. <sup>d</sup> Determined by DSC.

**Table 3** Ethylene polymerization using **Ni1–Ni6/EASC**<sup>a</sup>

Entry	Pre-cat.	Al/Ni	<i>T</i> (°C)	<i>t</i> (min)	Yield (g)	Activity <sup>b</sup>	<i>M<sub>w</sub></i> <sup>c</sup>	<i>M<sub>w</sub></i> / <i>M<sub>n</sub></i> <sup>c</sup>	<i>T<sub>m</sub></i> <sup>d</sup> (°C)
1	<b>Ni6</b>	400	30	30	14.22	14.22	4.29	2.47	53.1
2	<b>Ni6</b>	500	30	30	16.23	16.23	3.89	2.25	44.4
3	<b>Ni6</b>	600	30	30	15.33	15.33	3.74	2.29	49.1
4	<b>Ni6</b>	700	30	30	17.45	17.45	3.68	2.38	50.9
5	<b>Ni6</b>	800	30	30	15.14	15.14	3.37	2.16	63.3
6	<b>Ni6</b>	900	30	30	12.60	12.60	3.07	2.22	91.1
7	<b>Ni6</b>	700	20	30	2.11	2.11	4.43	2.39	103.6
8	<b>Ni6</b>	700	40	30	7.72	7.72	2.89	1.97	51.3
9	<b>Ni6</b>	700	50	30	3.88	3.88	2.69	2.34	44.2
10	<b>Ni6</b>	700	30	5	2.17	13.04	2.99	2.14	79.4
11	<b>Ni6</b>	700	30	15	6.76	13.52	3.40	2.10	64.0
12	<b>Ni6</b>	700	30	45	20.10	13.40	4.15	2.38	56.7
13	<b>Ni6</b>	700	30	60	22.01	11.01	4.56	2.05	55.1
14	<b>Ni1</b>	700	30	30	6.64	6.64	4.51	2.25	78.7
15	<b>Ni2</b>	700	30	30	7.96	7.96	3.91	2.14	57.8
16	<b>Ni3</b>	700	30	30	11.06	11.06	3.85	2.20	56.4
17	<b>Ni4</b>	700	30	30	9.05	9.05	4.34	2.15	53.5
18	<b>Ni5</b>	700	30	30	12.20	12.20	4.24	1.87	41.5
19 <sup>e</sup>	<b>Ni6</b>	700	30	30	5.13	5.13	2.40	1.59	23.1
20 <sup>f</sup>	<b>Ni6</b>	700	30	30	1.15	1.15	4.52	1.99	60.6

<sup>a</sup> Conditions: 2.0 μmol of **Ni6**; 10 atm of ethylene; total volume 100 mL. <sup>b</sup> Activity: 10<sup>6</sup> g PE mol<sup>-1</sup> (Ni) h<sup>-1</sup>. <sup>c</sup> *M<sub>w</sub>*: 10<sup>5</sup> g mol<sup>-1</sup>; *M<sub>w</sub>* and *M<sub>w</sub>*/*M<sub>n</sub>* determined by GPC. <sup>d</sup> Determined by DSC. <sup>e</sup> 5 atm. <sup>f</sup> 1 atm.

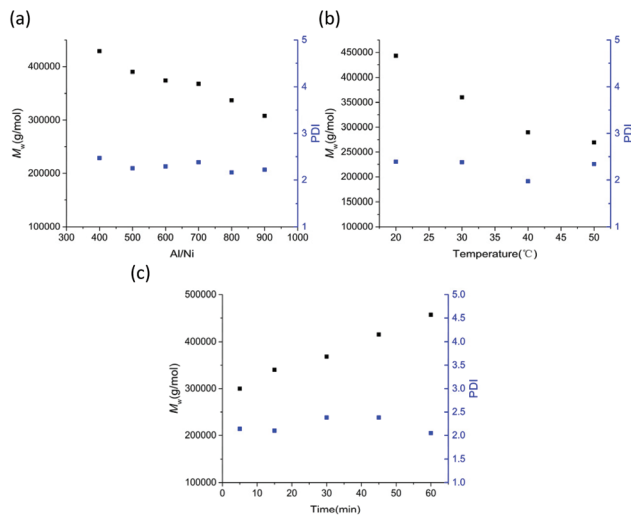


**Fig. 5** Molecular weight ( $M_w$ ) and PDI versus (a) molar ratio of Al/Ni (b) reaction temperature and (c) reaction time using Ni6/EASC.

20 and 50 °C (entries 4–9, Table 3) with the Al/Ni ratio fixed at 700 and the reaction time at 30 minutes. Inspection of the data reveals the optimum temperature in terms of catalytic activity to be 30 °C (entry 4, Table 2). As the temperature is increased above 30 °C the activity steadily decreases, an observation that can be accredited to the partial deactivation of the active species; similar results have been seen with related precatalysts.<sup>7a,12a,16c</sup> Indeed, the capacity of the *N*-aryl moieties to freely rotate at elevated temperature, resulting in increased associative displacement and/or C–H activation, has been suggested as a reason behind this lowering in activity noted in previously reported  $\alpha$ -diimine-nickel catalysts.<sup>4d</sup> With regard to the molecular weight of the polyethylene, this was found to decrease as the reaction temperature was raised from 20 to 50 °C, in accordance with more facile chain transfer and termination (see Fig. 5b). Notably, the lowest temperature run at 20 °C afforded polymer displaying the highest melting temperature ( $T_m$ ) of 103.6 °C consistent with more linear properties of this sample.

Thirdly, the lifetime of the catalyst was examined by determining the catalytic activity at 5, 15, 30, 45 and 60 minutes. Examination of the data reveals the maximum activity to occur after 30 minutes ( $17.45 \times 10^6$  g PE mol<sup>-1</sup> (Ni) h<sup>-1</sup>) and then steadily decrease over the second 30 minutes (entries 4 and 10–13, Table 3). The lower activities observed in the 5–15 minutes timeframe can be ascribed to the induction period required to fully generate the active species. Beyond 30 minutes, the activity drops from its maximum to a level of  $11.01 \times 10^6$  g PE mol<sup>-1</sup> (Ni) h<sup>-1</sup> after 60 minutes with the onset of catalyst deactivation. Nevertheless, despite this apparent catalyst decay this still represents good activity and highlights the stability of this catalyst. With regard to the molecular weight this increases over the duration of the test (see Fig. 5c) with the resultant polyethylenes showing narrow polydispersity (PDI range: 1.97–2.38) in accord with a single site active species.

When the pressure of ethylene was lowered from 10 to 1 atmospheres, the activity also dropped which can be attributed to mass transport limitations of the monomer at this low ethylene concentration.<sup>4d</sup>

Based on the above results using Ni6/EASC, the optimum conditions were identified as: Al/Ni molar ratio of 700, 30 °C reaction temperature and a run time of 30 minutes. To establish the relationship between structural variations in the precatalyst and catalytic performance in ethylene polymerization, the remaining complexes (Ni1–Ni5) were also investigated using these conditions (entries 14–18, Table 3). All the complexes exhibited good activities in the range  $6.64$ – $17.45 \times 10^6$  g PE mol<sup>-1</sup> (Ni) h<sup>-1</sup> with the overall order being Ni6 (2-cyclooctyl-4,6-methyl) > Ni5 (2-cyclopentyl-4,6-methyl) > Ni3 (2-cyclooctyl-6-methyl) > Ni4 (2-cyclohexyl-4,6-methyl) > Ni2 (2-cyclopentyl-6-methyl) > Ni1 (2-cyclohexyl-6-methyl). In terms of the particular 4-R group, Ni3 (2-cyclooctyl-6-methyl) > Ni2 (2-cyclopentyl-6-methyl) > Ni1 (2-cyclohexyl-6-methyl) for R = H while for R = Me, Ni6 (2-cyclooctyl-4,6-methyl) > Ni5 (2-cyclopentyl-4,6-methyl) > Ni4 (2-cyclohexyl-4,6-methyl). Several points emerge from examination of these findings. Firstly, the type of cycloalkyl group positioned at the *ortho*-position of the *N*-aryl group affects catalytic activity with the largest ring system, cyclooctyl giving the highest activities (Ni6, Ni3). Somewhat surprisingly the smaller cyclopentyl-systems (Ni5, Ni2) are more active than their cyclohexyl counterparts (Ni4, Ni1). Secondly, the nature of the 4-R group is also influential on catalytic activity with 4-Me derivatives more active than their 4-H analogues. To explain the superior performance of the cyclooctyl systems it would seem plausible that the flexible conformation of the cyclooctyl ring can protect the metal center in the active catalyst but not impede the approach of the ethylene monomer. By contrast, the protection of active species with the cyclohexyl and cyclopentyl would appear less effective. The positive effect on catalytic activity imposed by the presence of a *para*-methyl group (Ni4, Ni5 and Ni6) has some precedent and is likely due to its the electron donating properties and influence on the active species.<sup>3a,17</sup>

**Optimization and evaluation of Ni1–Ni6/MMAO.** In a manner similar to that described with EASC, this time using MMAO as the co-catalyst and Ni6 as the precatalyst, we set about again optimizing the reaction conditions and exploring the effects on the polymer properties; the data are collected in Table 3. In general, catalysts based on Ni6/MMAO when compared with Ni6/EASC, exhibit similarly high activity but display higher molecular weights as well as broader PDIs and higher  $T_m$  values.

On varying the molar ratio of Al/Ni from 1000 to 3000, the activity increased to a peak of  $10.93 \times 10^6$  g PE mol<sup>-1</sup> (Ni) h<sup>-1</sup> with the ratio at 2000 and then decreased (entries 1–7, Table 4). In addition, the polyethylenes obtained with different molar equivalents of MMAO showed a slight variation in polydispersity, while the molecular weight generally lowered on raising the molar ratio (Fig. 6a).

With respect to the effect of temperature, we carried out the polymerization at 20, 30, 40 and 50 °C (entries 4 and 8–10, Table 4). Once again 30 °C was found to be the optimum temp-

Table 4 Ethylene polymerization using Ni1–Ni6/MMAO<sup>a</sup>

Entry	Pre-cat.	Al/Ni	T (°C)	t (min)	Yield (g)	Activity <sup>b</sup>	M <sub>w</sub> <sup>c</sup>	M <sub>w</sub> /M <sub>n</sub> <sup>c</sup>	T <sub>m</sub> <sup>d</sup> (°C)
1	Ni6	1000	30	30	6.22	6.22	5.99	2.61	80.0
2	Ni6	1500	30	30	6.72	6.72	5.73	2.40	78.1
3	Ni6	1750	30	30	7.10	7.10	5.52	2.58	72.8
4	Ni6	2000	30	30	10.93	10.93	4.91	2.22	66.5
5	Ni6	2250	30	30	9.12	9.12	4.82	2.63	73.1
6	Ni6	2500	30	30	6.11	6.11	4.67	2.66	73.0
7	Ni6	3000	30	30	5.83	5.83	4.58	2.89	74.2
8	Ni6	2000	20	30	6.57	6.57	6.68	3.08	99.1
9	Ni6	2000	40	30	5.32	5.32	4.76	2.60	64.6
10	Ni6	2000	50	30	3.91	3.91	3.47	2.19	45.6
11	Ni6	2000	30	5	2.21	13.24	3.90	2.50	70.7
12	Ni6	2000	30	15	5.32	10.64	4.93	2.85	69.8
13	Ni6	2000	30	45	14.67	9.77	4.52	2.41	64.2
14	Ni6	2000	30	60	16.71	8.35	2.14	2.01	75.9
15	Ni1	2000	30	30	3.92	3.92	4.16	2.28	56.6
16	Ni2	2000	30	30	4.21	4.21	3.95	2.09	70.9
17	Ni3	2000	30	30	4.92	4.92	5.79	2.39	69.5
18	Ni4	2000	30	30	5.07	5.07	4.82	2.10	66.6
19	Ni5	2000	30	30	8.20	8.20	3.96	2.41	61.6
20 <sup>e</sup>	Ni6	2000	30	30	4.21	4.21	2.67	1.89	30.7
21 <sup>f</sup>	Ni6	2000	30	30	0.56	0.56	4.81	2.51	70.3

<sup>a</sup> Conditions: 2.0 μmol of Ni6; 10 atm of ethylene; total volume 100 mL. <sup>b</sup> Activity: ×10<sup>6</sup> g PE mol<sup>-1</sup> (Ni) h<sup>-1</sup>. <sup>c</sup> M<sub>w</sub>: ×10<sup>5</sup> g mol<sup>-1</sup>; M<sub>w</sub> and M<sub>w</sub>/M<sub>n</sub> determined by GPC. <sup>d</sup> Determined by DSC. <sup>e</sup> 5 atm. <sup>f</sup> 1 atm.

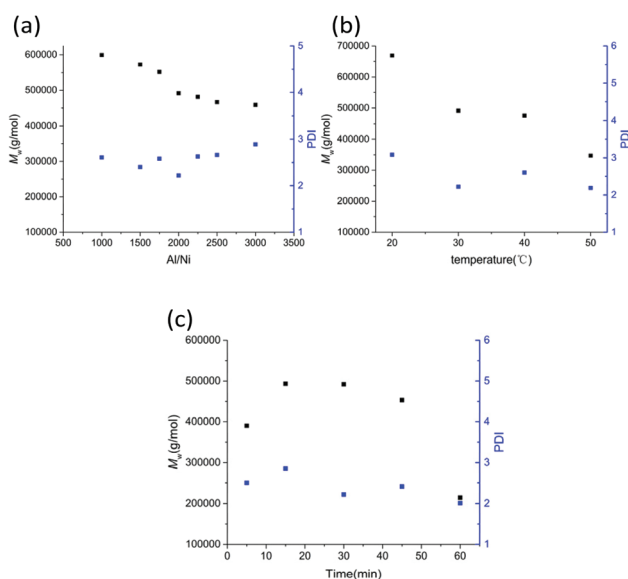


Fig. 6 Molecular weight ( $M_w$ ) and PDI versus (a) molar ratio of Al/Ni (b) run temperature and (c) reaction time using Ni6/MMAO.

erature in line with that observed with EASC. Over the temperature range the molecular weight of the polyethylene was found to decrease as the reaction temperature was increased in agreement with more facile chain transfer and termination (Fig. 6b). The lowest temperature run at 20 °C afforded polymers displaying the highest  $T_m$  values characteristic of more linear properties of the polymer.

Unlike with EASC, the MMAO-promoted polymerization displayed the highest activity after 5 minutes which was up to

13.24 × 10<sup>6</sup> g PE mol<sup>-1</sup> (Ni) h<sup>-1</sup> (entries 4 and 11–14, Table 4) highlighting the fast induction period of this particular catalyst. Beyond 5 minutes the activity gradually decreases reaching its lowest value of 8.35 × 10<sup>6</sup> g PE mol<sup>-1</sup> (Ni) h<sup>-1</sup> (entry 14, Table 4) after 60 minutes representing a 37% decrease. In terms of the PDI, a slightly wider variation with time (range: 2.01–2.85) was displayed when compared to that observed with EASC, while the molecular weights increased to a maximum between 15 and 30 minutes and then gradually decreased (Fig. 6c).

With the optimal conditions established for Ni6/MMAO, with the Al/Ni molar ratio set at 2000, the temperature at 30 °C and a run time of 30 minutes, Ni1–Ni5 were screened using these conditions (entries 4 and 15–19, Table 4). As with the EASC study, Ni6/MMAO showed the highest activity; albeit less than with Ni6/EASC. Likewise, the correlation between the activities of all the complexes showed a similar trend, Ni6 (2-cyclooctyl-4,6-methyl) > Ni5 (2-cyclopentyl-4,6-methyl) > Ni4 (2-cyclohexyl-4,6-methyl) > Ni3 (2-cyclooctyl-6-methyl) > Ni2 (2-cyclopentyl-6-methyl) > Ni1 (2-cyclohexyl-6-methyl) with the exception that Ni4 and Ni3 exchange places. On the basis of the R group, however, the trend was identical to that seen for EASC. Hence for R = H, Ni3 (2-cyclooctyl-6-methyl) > Ni2 (2-cyclopentyl-6-methyl) > Ni1 (2-cyclohexyl-6-methyl), while with R = Me the order is Ni6 (2-cyclooctyl-4,6-methyl) > Ni5 (2-cyclopentyl-4,6-methyl) > Ni4 (2-cyclohexyl-4,6-methyl). Once again this study highlights the important role played by the cyclooctyl group in affecting catalytic activity which is supplemented by the presence of a *para*-methyl group.

**Polyethylene microstructures.** Inspection of the two sets of polymerization data (Tables 3 and 4), reveals the  $T_m$  values of the polymers obtained in the runs performed at 30 °C or above

to be under 80 °C suggesting a high branching content.<sup>12a,16c,18</sup> To verify this, high temperature <sup>13</sup>C NMR spectroscopy was performed on the sample obtained using the more active catalysts Ni6/EASC (entry 4, Table 3) and Ni6/MMAO at 30 °C (entry 4, Table 4) and compared with the data obtained at 50 °C (entry 9, Table 3 and entry 10, Table 4). The NMR signals were assigned on the basis of previously reported characterization data.<sup>18b</sup> The polyethylene generated using Ni6/EASC at 30 °C (Fig. 7) contains 113 branches/1000 carbons, with the predominant types being methyl (64%), ethyl (5.5%), propyl (7.5%), butyl (2.0%) and longer chains (21%). Comparatively, the polymer obtained using Ni6/MMAO at 30 °C (Fig. 8) displays 89 branches/1000 carbons, with the main types of branches being only methyl (72%) and longer chain branches (28%). The higher degree of branching with Ni6/EASC over Ni6/MMAO at this run temperature is also consistent with the lower observed *T<sub>m</sub>* values (50.9 vs. 66.5 °C, respectively).

By contrast, the polymer obtained at 50 °C for Ni6/EASC (Fig. 9) shows a higher branching content at 134 branches/1000 carbons. In comparison with that at obtained at 30 °C the content of methyl-type branches increases from 64 to 67%, while the percentage of longer chain branches decreases from 21 to 12%. For the polymer obtained using Ni6/MMAO at 50 °C (Fig. 10), the total branching content is also higher at 122 branches/1000 carbons. However, the resulting polymers display a different distribution of branches over the temperature range. At 50 °C, the content of methyl-type branches using Ni6/MMAO decreases from 72 to 67% and the longer chain branches lowers from 28 to 10%, while the short chain branches, including ethyl, propyl, butyl and amyl branches, increase from zero to 9.5%, 8.5%, 4.0%, 1.0%, respectively. Overall, raising the temperature of the polymerization run leads to an increase in the branching content with the result that the polymer becomes less crystalline and more amorphous.

**Mechanical properties of the polyethylenes.** Given the observed branching content of the polyethylenes, a selection

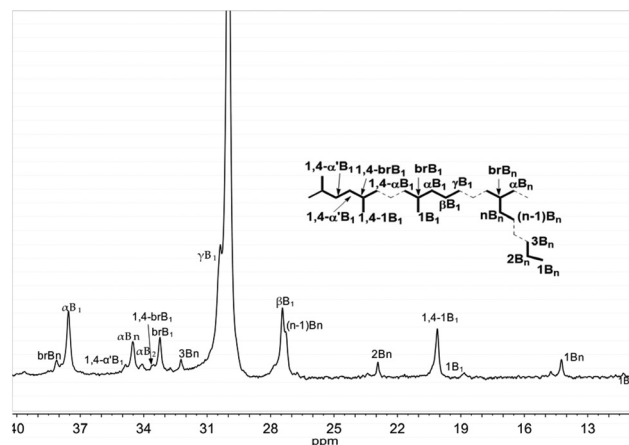


Fig. 8 <sup>13</sup>C NMR spectrum of the polyethylene sample obtained using Ni6/MMAO at 30 °C (entry 4, Table 4).

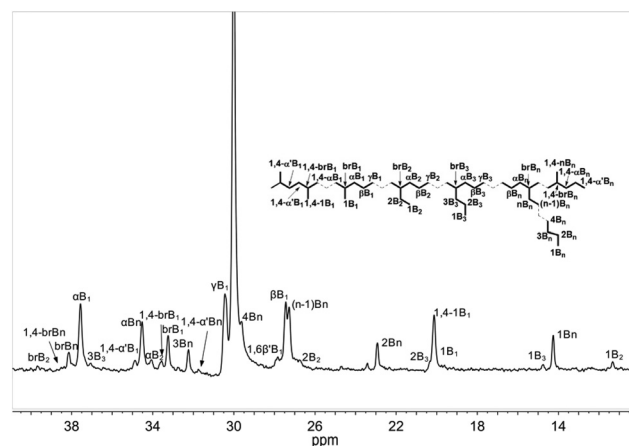


Fig. 9 <sup>13</sup>C NMR spectrum of the polyethylene sample obtained using Ni6/EASC at 50 °C (entry 9, Table 3).

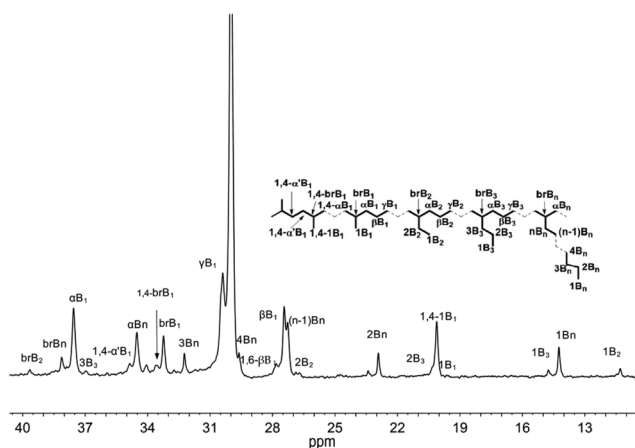


Fig. 7 <sup>13</sup>C NMR spectrum of the polyethylene sample obtained using Ni6/EASC at 30 °C (entry 4, Table 3).

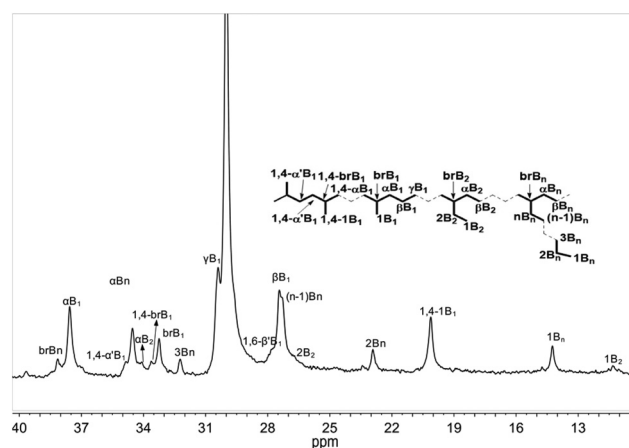


Fig. 10 <sup>13</sup>C NMR spectrum of the polyethylene sample obtained using Ni6/MMAO at 50 °C (entry 10, Table 4).

of samples was used to assess their mechanical properties and in turn their elastomeric properties. A total of eight samples were selected, four derived from Ni6/EASC and four from Ni6/MMAO each obtained at four different temperatures (20, 30, 40, 50 °C). The samples, designated, EASC-20, EASC-30, EASC-40, EASC-50 (entries 7, 4, 8 and 9, Table 3), MMAO-20, MMAO-30, MMAO-40 and MMAO-50 (entries 8, 4, 9 and 10, Table 4) were then subjected to stress–strain testing and dynamic mechanical analysis (DMA) (Table 5).<sup>19</sup>

Firstly, the monotonic tensile stress–strain data were recorded on all samples. Each mechanical test was performed with an average of five specimens at 30 °C with 70% air humidity. For the EASC samples, the lowest ultimate tensile strength (1.75 MPa) and strain at break (252.2%) was observed by EASC-50, which can be ascribed to it being almost amorphous (Fig. 11). Indeed, this sample shows the lowest  $X_c$  at 0.1%, the lowest  $T_m$  at 44.2 °C and the lowest melting enthalpy ( $\Delta H_m$ ) of the series at 0.3 J g<sup>-1</sup> (cf. 88 J g<sup>-1</sup> for EASC-20).<sup>20</sup> On increasing the crystallinity from 0.12% (EASC-50) to 9.70% (EASC-30), the ultimate tensile stress and elongation at break also increase from 0.12 to 9.70 MPa and 252.2 to 590.0%, respectively. Conversely, the most crystalline sample EASC-20 ( $X_c = 35.5\%$ ,  $T_m = 106.6$  °C) displays the opposite trend, with the ultimate tensile stress increasing but the elongation at break sharply decreasing. With regard to the samples obtained using MMAO, similar features are evident but in general exhibit comparatively higher crystallinity [ $X_c = 6.56\%$  MMAO-50, 16.7% MMAO-40, 22.9% MMAO-30] with the effect that the ultimate tensile stress data is also relatively higher. As evidenced by these stress–strain tests, the polymers obtained at higher temperature show better elastomeric properties which can be attributed to their higher branching content.<sup>21</sup> In general, the degree of stretching relates to the crystallinity ( $X_c$ ) and to some degree the molecular weight with the upshot that elasticity is mainly caused by low crystallinity.<sup>22</sup> The environmental scanning electron micrographs (ESEM) of EASC-30 and EASC-50 shown in Fig. 12 further highlight the effects of temperature on the crystallinity, in this case by the assessment of the fracture appearance. Sample EASC-30 shows a smoother fracture surface owing to its relatively higher crys-

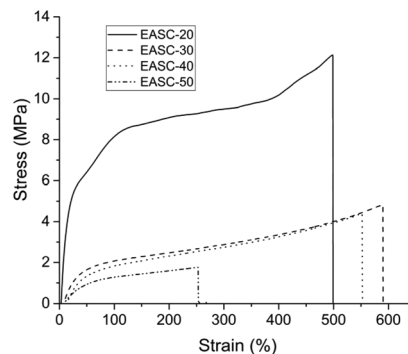


Fig. 11 Stress–strain curves for EASC-20, EASC-30, EASC-40 and EASC-50; the end points of the curves correspond to tensile failure of the samples.

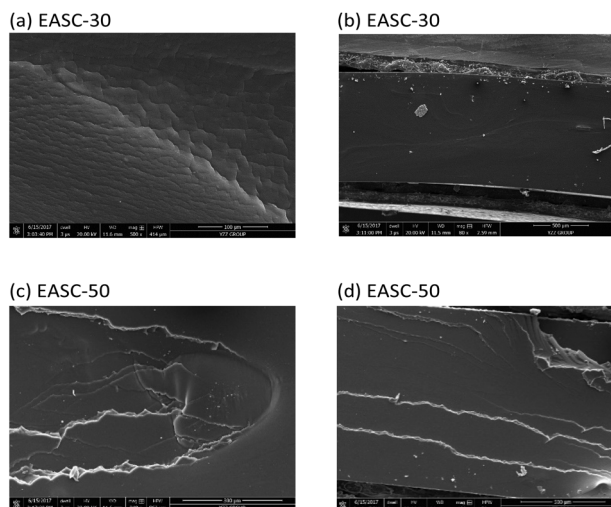


Fig. 12 ESEM of EASC-30 (top) and EASC-50 (bottom) at different magnifications: (a) 100, (b) 500, (c) 300 and (d) 500.

Table 5 Selected properties of EASC-20 to EASC-50 and MMAO-20 to MMAO-50

Sample	$T$ (°C)	$T_m^a$ (°C)	$M_w^b$	$X_c^a$ (%)	Stress <sup>c</sup> (MPa)	Strain <sup>c</sup> (%)
EASC-20	20	103.6	4.43	35.5	12 ± 0.7	498 ± 8
EASC-30	30	50.9	3.60	9.70	4.8 ± 0.9	590 ± 72
EASC-40	40	51.3	2.89	4.53	2.1 ± 0.7	552 ± 43
EASC-50	50	44.2	3.26	0.12	1.8 ± 0.3	252 ± 64
MMAO-20	20	99.1	6.68	29.5	8.0 ± 0.5	131 ± 54
MMAO-30	30	66.5	4.91	22.9	5.7 ± 0.2	481 ± 13
MMAO-40	40	64.6	4.76	16.7	3.9 ± 0.4	469 ± 58
MMAO-50	50	45.6	3.47	6.56	2.5 ± 0.4	402 ± 46

<sup>a</sup> Determined by DSC;  $X_c = \Delta H_f(T_m) / \Delta H_f^\circ(T_m^\circ)$ ;  $\Delta H_f^\circ(T_m^\circ) = 248.3$  J g<sup>-1</sup>.<sup>20</sup>

<sup>b</sup>  $M_w$ :  $\times 10^5$  g mol<sup>-1</sup>; determined by GPC. <sup>c</sup> Determined using a universal tester.

tallinity while the fracture becomes rougher in EASC-50 with additional deformation evident on account of its decreased crystallinity.

Secondly, the stress–strain recovery tests were also performed on the polymer samples. Specifically, the data were collected at –10 °C and 30 °C using all eight samples by dynamic mechanical analysis (DMA) (Fig. 13). Each recovery test involves 10 cycles to allow testing for elastic extenuation. Samples EASC-20 and MMAO-20 were found too stiff to stretch, with the result that they went beyond the stretch limit of the instrument. Nonetheless, these findings further support that these particular polymers are more linear hence display a higher crystalline content. On the other hand, the other samples behaved satisfactorily in the test and showed that the elastic recovery decreased relatively little whilst maintaining good elasticity even after 10 cycles. For EASC-30, EASC-40, and EASC-50, as the temperature was increased from –10 to 30 °C, the elastic recovery increased from 40.7 to 66.6%, 41.7 to 70.4%, 43.5 to 75.5%, respectively. Conversely, the Young's

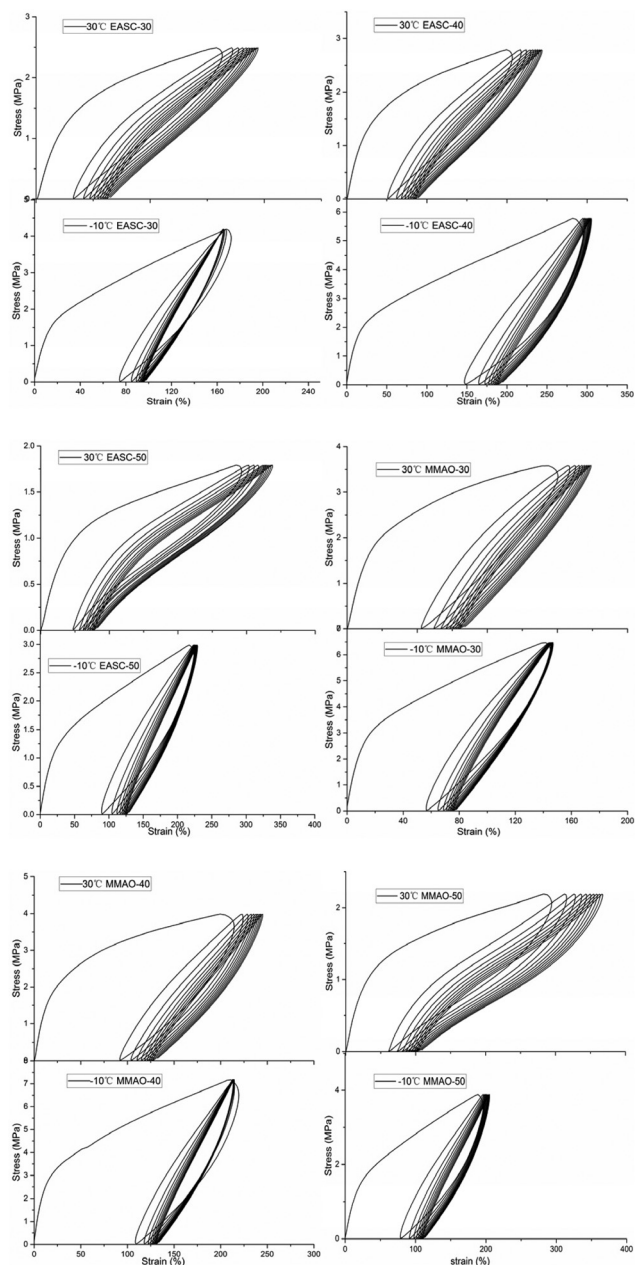


Fig. 13 Stress–strain recovery tests for EASC-30, EASC-40, EASC-50, MMAO-30, MMAO-40 and MMAO-50 at  $-10\text{ }^{\circ}\text{C}$  and  $30\text{ }^{\circ}\text{C}$ .

moduli for the corresponding samples decreased sharply from 12.4 MPa to 5.96 MPa, 12.3 MPa to 5.32 MPa and 6.85 MPa to 2.93 MPa. In the same way, the MMAO samples, MMAO-30, MMAO-40 and MMAO-50, exhibited similar trends and comparable elastic recovery with the elastic recovery increasing from 47.0 to 51.8%, 47.6 to 56.0% and 48.8 to 70.4%, respectively, while the Young's moduli dropped from 23.4 MPa to 11.3 MPa, 21.8 MPa to 10.5 MPa and 9.28 MPa to 4.53 MPa.

With specific regard to MMAO-30, the elastic recovery for the 1<sup>st</sup> cycle obtained at either  $-10\text{ }^{\circ}\text{C}$  or  $30\text{ }^{\circ}\text{C}$  resembles that observed at the 10<sup>th</sup> cycle at the same two temperatures (Fig. 14). At  $-10\text{ }^{\circ}\text{C}$ , the elastic recovery at the 10<sup>th</sup> cycle was

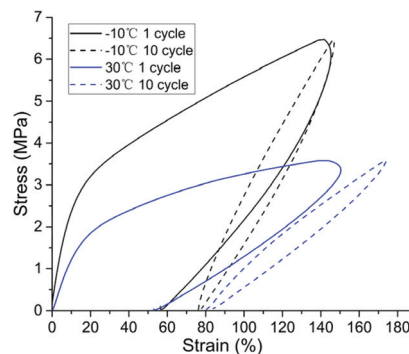


Fig. 14 Stress–strain recovery tests for the 1<sup>st</sup> and 10<sup>th</sup> cycle for MMAO-30 at  $-10\text{ }^{\circ}\text{C}$  and  $30\text{ }^{\circ}\text{C}$ .

found to be 43.5% which compares with 61.2% at the 1<sup>st</sup> cycle. Similarly at  $30\text{ }^{\circ}\text{C}$ , the value lowered from 64.8% (1<sup>st</sup> cycle) to 51.8% (10<sup>th</sup> cycle) highlighting the gradual loss in elasticity after being stretched multiple times. All the data show a temperature dependence, which indicates that the elastic properties in this case are more likely influenced by crystallinity than by molecular weight or molecular weight distribution.<sup>2,3</sup> In comparison with our previous findings the specimens generated in this study, with one exception,<sup>1,2a</sup> exhibit higher elastic recovery as well as larger Young's moduli. The improvement in Young's modulus makes the elastomers stronger and more resistant to external damage which broadens the application of these materials. Once again this reinforcement can be attributed to the increased degree of crystallinity.<sup>2,4</sup>

## Conclusions

A range of distinct 4-R-2-methyl-6-cycloalkyl-substituted aryl groups (cycloalkyl = cyclopentyl, cyclohexyl or cyclooctyl and R = Me or H) have been successfully integrated into an unsymmetrical diaryliminoacene ligand frame allowing access to the nickel(II) bromide complexes, **Ni1–Ni6**. All complexes and ligands have been characterized by a combination of NMR and FTIR spectroscopy as well as by elemental analysis; single crystal X-ray diffraction studies have been performed on **Ni1**, **Ni2**, **Ni3** and **Ni5**. On activation with EASC and MMAO, all the complexes displayed high activities towards ethylene polymerization between  $20\text{--}50\text{ }^{\circ}\text{C}$  with the *ortho*-substituted cyclooctyl systems (**Ni6**, **Ni3**) proving more active than the cyclopentyl (**Ni5**, **Ni2**) and cyclohexyl (**Ni4**, **Ni1**) counterparts for a given R group. Moreover, the branching content of the polymers could be influenced by the temperature of the polymerization run with hyperbranched materials accessible at the higher temperatures. The mechanical and elasticity properties of these materials have been thoroughly investigated and reveal features comparable with thermoplastic elastomers. Compared with previously work conducted by the Sun<sup>7a</sup> and Ivanchev groups,<sup>8d</sup> this work has some advantages in terms of higher catalytic activities and lower  $T_m$  values for the polymers.

## Experimental

### General considerations

All manipulations of air- and/or moisture-sensitive compounds were carried out under a nitrogen atmosphere using standard Schlenk techniques. Toluene was refluxed over sodium benzo-phenone and distilled under nitrogen prior to use. Methylaluminoxane (MAO, 1.46 M solution in toluene) and modified methylaluminoxane (MMAO, 2.0 M in heptane, 3A) were purchased from Akzo Nobel Corp. Diethylaluminum chloride ( $\text{Et}_2\text{AlCl}$ , 1.17 M in toluene) and ethylaluminum sesquichloride ( $\text{Et}_3\text{Al}_2\text{Cl}_3$ , EASC, 0.87 M in toluene) were purchased from Acros Chemicals. High-purity ethylene was purchased from Beijing Yansan Petrochemical Co. and used as received. Other reagents were purchased from Aldrich, Acros or local suppliers. NMR spectra were recorded on a Bruker DMX 400 MHz instrument at ambient temperature using TMS as an internal standard;  $\delta$  values are given in ppm and  $J$  values in Hz. IR spectra were recorded on a PerkinElmer System 2000 FT-IR spectrometer. Elemental analysis was carried out using a Flash EA 1112 microanalyzer. Molecular weights and molecular weight distributions (MWD) of the polyethylene were determined using a PL-GPC220 instrument at 150 °C, with 1,2,4-trichlorobenzene as the solvent. Melting points of the polyethylenes were measured from the second scanning run on a PerkinElmer DSC-7 differential scanning calorimeter (DSC) under a nitrogen atmosphere; in the procedure, a sample of about 5.0 mg was heated to 150 °C at a rate of 10 °C  $\text{min}^{-1}$  and kept for 5 min at 150 °C to remove the thermal history and then cooled at a rate of 10 °C  $\text{min}^{-1}$  to -20 °C.  $^{13}\text{C}$  NMR spectra of the polyethylenes were recorded on a Bruker DMX-300 MHz instrument at 135 °C in deuterated 1,1,2,2-tetrachloroethane with TMS as an internal standard. The stress-strain curves were obtained using a universal tester (Instron 1122, UK), while the ESEM measurements was undertaken using an environmental scanning electron microscope (Quanta feg200) at 20 kV. The stress-strain recovery tests at different temperatures were carried out using a dynamic mechanical analyzer (DMA 800, TA) under controlled force mode. 2,6-Dibenzhydryl-4-methylaniline, 2-cyclohexyl-6-methylaniline hydrochloride, 2-cyclopentyl-6-methylaniline hydrochloride, 2-cyclooctyl-6-methylaniline hydrochloride, 2-cyclohexyl-4,6-dimethylaniline hydrochloride, 2-cyclopentyl-4,6-dimethylaniline hydrochloride, 2-cyclooctyl-4,6-dimethylaniline hydrochloride, have been prepared using literature methods.<sup>8g</sup>

### Synthesis and characterization

**2-(2,6-Dibenzhydryl-4-methylphenylimino)acenaphthylene.** A mixture of 2,6-dibenzhydryl-4-methylphenylamine (8.78 g, 20.0 mmol) and acenaphthylene-1,2-dione (3.64 g, 20.0 mmol) was dissolved in dichloromethane (200 mL) and a catalytic amount of *p*-toluenesulfonic acid in ethanol (10 mL) added. After stirring overnight in room temperature, the solvent was removed under reduced pressure and the residue purified by column chromatography on alumina with petroleum ether/dichloromethane (1/1 v/v) as the eluent. Following solvent

removal and drying under reduced pressure, the product was isolated as an orange solid (8.68 g, 72%).  $^1\text{H}$  NMR (400 MHz,  $\text{CDCl}_3$ , TMS):  $\delta$  8.04 (t,  $J$  = 7.8 Hz, 2H), 7.76 (m, 2H), 7.27 (s, 1H), 7.24 (s, 2H), 7.19 (d,  $J$  = 7.1 Hz, 2H), 7.08 (d,  $J$  = 7.2 Hz, 5H), 6.88 (d,  $J$  = 7.3 Hz, 4H), 6.81 (s, 3H), 6.61 (t,  $J$  = 7.5 Hz, 4H), 6.44 (t,  $J$  = 7.3 Hz, 2H), 6.15 (d,  $J$  = 7.1 Hz, 1H), 5.45 (s, 2H), 2.28 (s, 3H).  $^{13}\text{C}$  NMR (101 MHz,  $\text{CDCl}_3$ , TMS):  $\delta$  189.91, 162.50, 146.08, 143.11, 142.61, 141.91, 133.36, 131.94, 131.89, 129.83, 129.59, 128.84, 128.54, 128.29, 127.93, 127.13, 126.33, 125.64, 124.06, 121.67, 52.29, 21.67. IR (KBr;  $\text{cm}^{-1}$ ): 3026 (w), 1722 ( $\nu_{\text{C=O}}$ , s), 1650 ( $\nu_{\text{C=N}}$ , m), 1596 (s), 1489 (s), 1446 (s), 1269 (m), 1268 (w), 1026 (s), 908 (m), 827 (m), 774 (s), 745 (s). Anal. calcd for  $\text{C}_{45}\text{H}_{33}\text{NO}$  (603.77): C, 89.52; H, 5.51; N, 2.32. Found: C, 89.22; H, 5.67; N, 2.29.

### Synthesis of L1-L6

**1-{2,6-(Ph<sub>2</sub>CH)<sub>2</sub>-4-MeC<sub>6</sub>H<sub>2</sub>N}-2-{2-(C<sub>6</sub>H<sub>11</sub>)-6-MeC<sub>6</sub>H<sub>3</sub>N}C<sub>2</sub>C<sub>10</sub>H<sub>6</sub> (L1).** A solution of 2-(2,6-dibenzhydryl-4-methylphenylimino)acenaphthylene (1.206 g, 2.0 mmol), 2-cyclohexyl-6-methylphenylamine hydrochloride (0.450 g, 2.0 mmol) and a catalytic amount of *p*-toluenesulfonic acid in toluene (50 mL) were stirred and heated to reflux for 16 h. After removal of the volatiles under reduced pressure, the residue was purified by alumina column chromatography with petroleum ether/dichloromethane (1/1 v/v) as the eluent to afford L1 as a yellow solid (0.29 g, 19%).  $^1\text{H}$  NMR (400 MHz,  $\text{CDCl}_3$ , TMS):  $\delta$  7.70 (d,  $J$  = 8.2 Hz, 1H), 7.50 (d,  $J$  = 8.2 Hz, 1H), 7.29 (m, 2H), 7.24 (s, 2H), 7.22 (s, 1H), 7.19 (d,  $J$  = 7.2 Hz, 4H), 7.15 (t,  $J$  = 4.7 Hz, 1H), 7.09 (d,  $J$  = 7.9 Hz, 2H), 7.00 (d,  $J$  = 7.2 Hz, 2H), 6.91 (d,  $J$  = 7.3 Hz, 2H), 6.86 (m, 2H), 6.81 (s, 1H), 6.55 (t,  $J$  = 7.8 Hz, 4H), 6.46 (d,  $J$  = 7.2 Hz, 1H), 6.39 (t,  $J$  = 7.7 Hz, 2H), 5.89 (d,  $J$  = 7.2 Hz, 1H), 5.68 (s, 1H), 5.64 (s, 1H), 2.86 (m, 1H), 2.32 (s, 3H), 2.17 (s, 3H), 2.03 (d,  $J$  = 14.5 Hz, 1H), 1.73 (d,  $J$  = 12.1 Hz, 1H), 1.57 (m, 2H), 1.52–1.45 (m, 2H), 1.40–1.24 (m, 2H), 1.15 (m, 2H).  $^{13}\text{C}$  NMR (101 MHz,  $\text{CDCl}_3$ , TMS):  $\delta$  162.32, 155.27, 148.39, 146.72, 143.75, 141.78, 139.97, 136.98, 135.67, 133.58, 132.80, 132.40, 129.86, 129.76, 129.62, 129.10, 128.75, 128.31, 128.12, 127.81, 127.74, 127.26, 126.99, 126.07, 125.59, 124.69, 124.43, 124.13, 122.28, 52.15, 38.94, 34.87, 33.58, 27.01, 26.80, 26.16, 21.64, 18.85. IR (KBr;  $\text{cm}^{-1}$ ): 3025 (w), 2923 (w), 1663 ( $\nu_{\text{C=N}}$ , m), 1643 ( $\nu_{\text{C=N}}$ , m), 1594 (m), 1494 (m), 1445 (s), 1235 (w), 1078 (m), 1034 (m), 923 (m), 857 (w), 828 (m), 765 (s), 741 (s). Anal. calcd for  $\text{C}_{58}\text{H}_{50}\text{N}_2$  (775.05): C, 89.88; H, 6.51; N, 3.61. Found: C, 89.90; H, 6.53; N, 3.57.

**1-{2,6-(Ph<sub>2</sub>CH)<sub>2</sub>-4-MeC<sub>6</sub>H<sub>2</sub>N}-2-{2-(C<sub>5</sub>H<sub>9</sub>)-6-MeC<sub>6</sub>H<sub>3</sub>N}C<sub>2</sub>C<sub>10</sub>H<sub>6</sub> (L2).** Using a similar procedure and molar ratios to that described for L1 but with 2-cyclopentyl-6-methylphenylamine hydrochloride as the amine, L2 was obtained as a yellow powder (0.15 g, 10%).  $^1\text{H}$  NMR (400 MHz,  $\text{CDCl}_3$ , TMS):  $\delta$  7.70 (d,  $J$  = 8.2 Hz, 1H), 7.53 (d,  $J$  = 8.3 Hz, 1H), 7.29 (m, 2H), 7.23 (s, 2H), 7.21 (d,  $J$  = 4.8 Hz, 2H), 7.18 (s, 1H), 7.16 (d,  $J$  = 3.2 Hz, 1H), 7.14 (s, 3H), 7.11 (d,  $J$  = 5.0 Hz, 2H), 7.08 (s, 1H), 6.97–6.86 (m, 5H), 6.80 (d,  $J$  = 10.0 Hz, 2H), 6.62 (t,  $J$  = 7.6 Hz, 2H), 6.56 (t,  $J$  = 7.6 Hz, 2H), 6.46 (t,  $J$  = 6.9 Hz, 2H), 6.40 (dd,  $J$  = 14.2, 6.8 Hz, 1H), 6.01 (d,  $J$  = 7.1 Hz, 1H), 5.62 (s, 2H), 3.25 (m, 1H), 2.28 (s, 3H), 2.20 (s, 3H), 2.16–2.08 (m, 1H), 1.82–1.42 (m, 7H).  $^{13}\text{C}$  NMR (101 MHz,  $\text{CDCl}_3$ , TMS):  $\delta$  163.57, 161.84,

148.94, 146.75, 143.50, 141.91, 141.81, 139.95, 134.22, 132.59, 132.29, 132.17, 129.81, 129.74, 129.55, 128.95, 128.85, 128.74, 128.57, 128.07, 127.83, 127.78, 127.66, 127.20, 126.87, 126.05, 125.54, 125.41, 124.48, 124.20, 124.02, 122.21, 52.17, 52.12, 40.33, 35.91, 33.76, 26.05, 21.53, 18.54. IR (KBr;  $\text{cm}^{-1}$ ): 3235 (w), 2947 (w), 1660 ( $\nu_{\text{C}=\text{N}}$ , m), 1640 ( $\nu_{\text{C}=\text{N}}$ , m), 1594 (m), 1493 (m), 1445 (m), 1257 (m), 1079 (m), 1033 (w), 921 (m), 853 (m), 828 (m), 766 (s), 740 (s). Anal. calcd for  $\text{C}_{57}\text{H}_{48}\text{N}_2$  (761.03): C, 89.96; H, 6.36; N, 3.68. Found: C, 89.98; H, 6.50; N, 3.52.

$1\text{-}\{2,6\text{-}(\text{Ph}_2\text{CH})_2\text{-}4\text{-MeC}_6\text{H}_2\text{N}\}\text{-}2\text{-}\{2\text{-}(\text{C}_8\text{H}_{15})\text{-}6\text{-MeC}_6\text{H}_3\text{N}\}\text{C}_2\text{C}_{10}\text{H}_6$  (**L3**). Using a similar procedure and molar ratios to that described for **L1** but with 2-cyclooctyl-6-methylphenylamine hydrochloride as the amine, **L3** was obtained as a yellow powder (0.24 g, 15%).  $^1\text{H}$  NMR (400 MHz,  $\text{CDCl}_3$ , TMS):  $\delta$  7.73 (d,  $J = 8.2$  Hz, 1H), 7.52 (d,  $J = 8.3$  Hz, 1H), 7.34–7.27 (m, 2H), 7.24 (s, 2H), 7.22 (s, 1H), 7.21–7.14 (m, 5H), 7.11 (d,  $J = 7.4$  Hz, 2H), 6.97 (d,  $J = 7.3$  Hz, 2H), 6.91 (t,  $J = 10.7$  Hz, 3H), 6.85 (d,  $J = 7.6$  Hz, 1H), 6.81 (s, 1H), 6.60 (t,  $J = 7.5$  Hz, 2H), 6.56–6.42 (m, 4H), 6.34 (t,  $J = 7.3$  Hz, 1H), 5.89 (d,  $J = 7.1$  Hz, 1H), 5.70 (s, 1H), 5.64 (d,  $J = 11.6$  Hz, 1H), 3.24–2.91 (m, 1H), 2.29 (s, 3H), 2.21 (d,  $J = 13.9$  Hz, 3H), 2.11–1.92 (m, 1H), 1.85 (m, 1H), 1.70 (s, 1H), 1.68–1.58 (m, 2H), 1.57–1.47 (m, 4H), 1.37–1.15 (m, 5H).  $^{13}\text{C}$  NMR (101 MHz,  $\text{CDCl}_3$ , TMS):  $\delta$  166.44, 162.21, 148.45, 146.79, 143.75, 143.64, 141.86, 141.76, 139.90, 135.55, 132.65, 132.26, 132.14, 129.83, 129.80, 129.74, 129.69, 129.57, 129.53, 129.44, 129.05, 128.78, 128.70, 128.59, 128.22, 128.13, 128.03, 127.72, 127.65, 127.16, 126.90, 126.02, 125.98, 125.52, 125.44, 124.59, 124.51, 124.32, 124.00, 122.17, 77.34, 77.02, 76.70, 52.11, 52.01, 38.89, 34.76, 33.50, 26.98, 26.93, 26.73, 26.09, 21.53, 18.72. IR (KBr;  $\text{cm}^{-1}$ ): 3025 (w), 2917 (m), 2851 (w), 1664 ( $\nu_{\text{C}=\text{N}}$ , m), 1643 ( $\nu_{\text{C}=\text{N}}$ , m), 1594 (m), 1494 (m), 1446 (s), 1252 (w), 1077 (m), 1034 (m), 923 (m), 857 (w), 828 (m), 765 (s), 741 (s). Anal. calcd for  $\text{C}_{60}\text{H}_{54}\text{N}_2$  (803.11): C, 89.73; H, 6.78; N, 3.49. Found: C, 89.68; H, 6.85; N, 3.47.

$1\text{-}\{2,6\text{-}(\text{Ph}_2\text{CH})_2\text{-}4\text{-MeC}_6\text{H}_2\text{N}\}\text{-}2\text{-}\{2\text{-}(\text{C}_6\text{H}_{11})\text{-}4,6\text{-Me}_2\text{C}_6\text{H}_2\text{N}\}\text{C}_2\text{C}_{10}\text{H}_6$  (**L4**). Using a similar procedure and molar ratios to that described for **L1** but with 2-cyclohexyl-4,6-dimethylphenylamine hydrochloride as the amine, **L4** was obtained as a yellow powder (0.24 g, 15%).  $^1\text{H}$  NMR (400 MHz,  $\text{CDCl}_3$ , TMS):  $\delta$  7.70 (d,  $J = 8.2$  Hz, 1H), 7.50 (d,  $J = 8.3$  Hz, 1H), 7.29 (d,  $J = 7.8$  Hz, 2H), 7.24 (s, 1H), 7.23–7.16 (m, 4H), 7.11 (d,  $J = 6.5$  Hz, 3H), 7.02 (d,  $J = 6.8$  Hz, 2H), 6.96 (s, 1H), 6.92 (d,  $J = 7.5$  Hz, 2H), 6.88 (s, 1H), 6.87–6.80 (m, 2H), 6.55 (m, 5H), 6.40 (t,  $J = 7.3$  Hz, 2H), 5.90 (d,  $J = 7.0$  Hz, 1H), 5.69 (s, 1H), 5.64 (s, 1H), 2.85 (m, 1H), 2.42 (s, 3H), 2.29 (s, 3H), 2.16 (s, 3H), 2.02 (d,  $J = 12.5$  Hz, 1H), 1.72 (t,  $J = 15.4$  Hz, 1H), 1.45 (m, 5H), 1.18 (m, 1H).  $^{13}\text{C}$  NMR (101 MHz,  $\text{CDCl}_3$ , TMS):  $\delta$  163.88, 162.35, 146.89, 145.96, 143.79, 143.68, 141.91, 141.81, 139.89, 135.38, 133.09, 132.59, 132.27, 132.18, 129.84, 129.81, 129.76, 129.58, 129.54, 129.07, 128.92, 128.70, 128.45, 128.01, 127.71, 127.63, 127.14, 126.86, 126.00, 125.96, 125.50, 125.42, 125.21, 124.28, 124.21, 122.18, 53.37, 52.13, 52.02, 38.88, 34.80, 33.51, 31.58, 27.03, 26.77, 26.15, 22.64, 21.51, 21.21, 18.60, 14.08. IR (KBr;  $\text{cm}^{-1}$ ): 3024 (w), 2922 (s), 2851 (m), 1655 ( $\nu_{\text{C}=\text{N}}$ , m), 1632 ( $\nu_{\text{C}=\text{N}}$ , m), 1595 (m), 1493 (m), 1443 (s), 1232 (m), 1075 (m), 1034 (m), 924 (m), 857 (m), 829 (m), 779 (s), 743 (s). Anal.

calcd for  $\text{C}_{59}\text{H}_{52}\text{N}_2$  (789.08): C, 89.81; H, 6.64; N, 3.55. Found: C, 89.95; H, 6.56; N, 3.49.

$1\text{-}\{2,6\text{-}(\text{Ph}_2\text{CH})_2\text{-}4\text{-MeC}_6\text{H}_2\text{N}\}\text{-}2\text{-}\{2\text{-}(\text{C}_5\text{H}_9)\text{-}4,6\text{-Me}_2\text{C}_6\text{H}_2\text{N}\}\text{C}_2\text{C}_{10}\text{H}_6$  (**L5**). Using a similar procedure and molar ratios to that described for **L1** but with 2-cyclopentyl-4,6-dimethylphenylamine hydrochloride as the amine, **L5** was obtained as a yellow powder (0.19 g, 16%).  $^1\text{H}$  NMR (400 MHz,  $\text{CDCl}_3$ , TMS):  $\delta$  7.73 (d,  $J = 8.2$  Hz, 1H), 7.63 (d,  $J = 8.2$  Hz, 1H), 7.31 (m, 2H), 7.23 (s, 2H), 7.21 (d,  $J = 4.8$  Hz, 2H), 7.18 (s, 1H), 7.16 (d,  $J = 3.2$  Hz, 1H), 7.14 (s, 3H), 7.11 (d,  $J = 5.0$  Hz, 2H), 7.08 (s, 1H), 6.97–6.86 (m, 5H), 6.80 (d,  $J = 10.0$  Hz, 2H), 6.62 (t,  $J = 7.6$  Hz, 2H), 6.56 (t,  $J = 7.6$  Hz, 2H), 6.01 (d,  $J = 7.1$  Hz, 1H), 5.71 (s, 1H), 5.67 (s, 1H), 3.33–3.14 (m, 1H), 2.42 (s, 3H), 2.28 (s, 3H), 2.21 (s, 3H), 1.83–1.20 (m, 8H).  $^{13}\text{C}$  NMR (101 MHz,  $\text{CDCl}_3$ , TMS):  $\delta$  163.64, 162.02, 146.83, 146.48, 143.56, 143.53, 141.95, 141.84, 139.95, 133.97, 133.12, 132.55, 132.32, 132.21, 129.83, 129.75, 129.58, 128.96, 128.90, 128.73, 128.65, 128.45, 128.07, 127.81, 127.78, 127.66, 127.19, 126.84, 126.04, 125.54, 125.41, 124.77, 124.20, 124.18, 122.24, 53.41, 52.18, 52.13, 40.33, 35.88, 33.73, 26.06, 21.53, 21.26, 18.45. IR (KBr;  $\text{cm}^{-1}$ ): 3654 (w), 2946 (s), 1660 ( $\nu_{\text{C}=\text{N}}$ , m), 1638 ( $\nu_{\text{C}=\text{N}}$ , m), 1594 (m), 1491 (s), 1438 (s), 1256 (m), 1081 (w), 1033 (w), 921 (m), 853 (m), 830 (m), 766 (s), 741 (s). Anal. calcd for  $\text{C}_{58}\text{H}_{50}\text{N}_2$  (775.05): C, 89.88; H, 6.50; N, 3.61. Found: C, 89.91; H, 6.47; N, 3.62.

$1\text{-}\{2,6\text{-}(\text{Ph}_2\text{CH})_2\text{-}4\text{-MeC}_6\text{H}_2\text{N}\}\text{-}2\text{-}\{2\text{-}(\text{C}_8\text{H}_{15})\text{-}4,6\text{-Me}_2\text{C}_6\text{H}_2\text{N}\}\text{C}_2\text{C}_{10}\text{H}_6$  (**L6**). Using a similar procedure and molar ratios to that described **L1** but with 2-cyclooctyl-4,6-dimethylphenylamine hydrochloride as the amine, **L6** was obtained as a yellow powder (0.20 g, 12%).  $^1\text{H}$  NMR (400 MHz,  $\text{CDCl}_3$ , TMS):  $\delta$  7.68 (d,  $J = 8.2$  Hz, 1H), 7.49 (t,  $J = 8.5$  Hz, 1H), 7.27 (s, 1H), 7.21 (d,  $J = 8.1$  Hz, 3H), 7.16 (dd,  $J = 13.1, 7.3$  Hz, 4H), 7.09 (d,  $J = 7.5$  Hz, 3H), 6.96 (d,  $J = 8.0$  Hz, 3H), 6.90 (d,  $J = 6.8$  Hz, 3H), 6.86–6.77 (m, 2H), 6.59 (dd,  $J = 15.9, 7.6$  Hz, 3H), 6.54–6.44 (m, 3H), 6.33 (t,  $J = 7.4$  Hz, 1H), 5.88 (d,  $J = 7.1$  Hz, 1H), 5.64 (d,  $J = 6.2$  Hz, 2H), 3.01 (m, 1H), 2.41 (s, 3H), 2.28 (s, 3H), 2.17 (s, 3H), 2.02–1.91 (m, 1H), 1.82 (dd,  $J = 18.8, 11.2$  Hz, 1H), 1.68 (s, 1H), 1.62–1.55 (m, 2H), 1.53–1.46 (m, 3H), 1.46–1.28 (m, 6H).  $^{13}\text{C}$  NMR (101 MHz,  $\text{CDCl}_3$ , TMS):  $\delta$  162.15, 146.84, 145.35, 143.91, 143.73, 141.97, 141.68, 139.85, 136.83, 132.96, 132.58, 132.29, 132.14, 129.83, 129.71, 129.61, 129.48, 129.03, 128.78, 128.67, 128.47, 127.99, 127.73, 127.60, 127.16, 126.87, 125.98, 125.93, 125.71, 125.56, 125.35, 124.32, 124.22, 122.04, 52.16, 51.77, 39.35, 33.06, 32.43, 27.70, 27.61, 25.87, 25.42, 25.30, 21.53, 21.28, 18.68. IR (KBr;  $\text{cm}^{-1}$ ): 3022 (w), 2923 (m), 2853 (m), 1656 ( $\nu_{\text{C}=\text{N}}$ , m), 1639 ( $\nu_{\text{C}=\text{N}}$ , m), 1597 (m), 1468 (m), 1442 (s), 1275 (m), 1036 (m), 926 (m), 859 (s), 828 (s), 779 (s), 742 (s). Anal. calcd for  $\text{C}_{61}\text{H}_{56}\text{N}_2$  (817.13): C, 89.66; H, 6.91; N, 3.43. Found: C, 89.61; H, 6.89; N, 3.50.

#### Synthesis of Ni1–Ni6

$1\text{-}\{2,6\text{-}(\text{Ph}_2\text{CH})_2\text{-}4\text{-MeC}_6\text{H}_2\text{N}\}\text{-}2\text{-}\{2\text{-}(\text{C}_6\text{H}_{11})\text{-}6\text{-MeC}_6\text{H}_2\text{N}\}\text{C}_2\text{C}_{10}\text{H}_6$   $\text{NiBr}_2$  (**Ni1**). **L1** (0.162 g, 0.21 mmol) and  $\text{NiBr}_2(\text{DME})$  (0.062 g, 0.20 mmol) were added to a Schlenk tube together with ethanol (2 mL) and dichloromethane (10 mL). The reaction mixture was stirred at room temperature overnight after which time diethyl ether (30 mL) was added to precipitate the complex. The precipitate was filtered, washed with diethyl

ether (3 × 15 mL) and dried under reduced pressure to give **Ni1** as a red powder (0.10 g, 49%). IR (KBr; cm<sup>-1</sup>): 3028 (w), 2922 (m), 2852 (m), 1645 (ν<sub>C=N</sub>, m), 1620 (ν<sub>C=N</sub>, m), 1582 (s), 1494 (m), 1448 (s), 1294 (m), 1032 (m), 827 (m), 772 (w), 748 (w). Anal. calcd for C<sub>58</sub>H<sub>50</sub>Br<sub>2</sub>N<sub>2</sub>Ni (993.55): C, 70.12; H, 5.07; N, 2.82. Found: C, 70.20; H, 4.88; N, 2.90.

[1-{2,6-(Ph<sub>2</sub>CH)<sub>2</sub>-4-MeC<sub>6</sub>H<sub>2</sub>N}-2-{2-(C<sub>5</sub>H<sub>9</sub>)-6-MeC<sub>6</sub>H<sub>2</sub>N}]C<sub>2</sub>C<sub>10</sub>H<sub>6</sub>]NiBr<sub>2</sub> (**Ni2**). Using a similar procedure and molar ratios to that described for **Ni1** but with **L2** as the ligand, **Ni2** was obtained as a red powder (0.13 g, 66%). IR (KBr; cm<sup>-1</sup>): 3020 (w), 2960 (w), 2359 (w), 1646 (ν<sub>C=N</sub>, m), 1620 (ν<sub>C=N</sub>, m), 1590 (s), 1579 (m), 1485 (s), 1433 (s), 1287 (m), 1021 (m), 815 (w), 764 (m), 729 (m). Anal. calcd for C<sub>57</sub>H<sub>48</sub>Br<sub>2</sub>N<sub>2</sub>Ni (979.53): C, 69.89; H, 4.94; N, 2.86. Found: C, 69.99; H, 4.85; N, 2.79.

[1-{2,6-(Ph<sub>2</sub>CH)<sub>2</sub>-4-MeC<sub>6</sub>H<sub>2</sub>N}-2-{2-(C<sub>8</sub>H<sub>15</sub>)-6-MeC<sub>6</sub>H<sub>3</sub>N}]C<sub>2</sub>C<sub>10</sub>H<sub>6</sub>]NiBr<sub>2</sub> (**Ni3**). Using a similar procedure and molar ratios to that described for **Ni1** but with **L3** as the ligand, **Ni3** was obtained as a red powder (0.18 g, 98%). IR (KBr; cm<sup>-1</sup>): 3030 (w), 2910 (m), 2353 (w), 1645 (ν<sub>C=N</sub>, m), 1619 (ν<sub>C=N</sub>, m), 1599 (s), 1578 (m), 1488 (s), 1445 (s), 1291 (m), 1034 (m), 820 (w), 769 (s), 743 (vs). Anal. calcd for C<sub>60</sub>H<sub>54</sub>Br<sub>2</sub>N<sub>2</sub>Ni (1036.64): C, 70.54; H, 5.33; N, 2.74. Found: C, 70.61; H, 5.32; N, 2.72.

[1-{2,6-(Ph<sub>2</sub>CH)<sub>2</sub>-4-MeC<sub>6</sub>H<sub>2</sub>N}-2-{2-(C<sub>6</sub>H<sub>11</sub>)-4,6-Me<sub>2</sub>C<sub>6</sub>H<sub>2</sub>N}]C<sub>2</sub>C<sub>10</sub>H<sub>6</sub>]NiBr<sub>2</sub> (**Ni4**). Using a similar procedure and molar ratios to that described for **Ni1** but with **L4** as the ligand, **Ni4** was obtained as a red powder (0.04 g, 20%). IR (KBr; cm<sup>-1</sup>):

3021 (w), 2927 (m), 2361 (w), 1645 (ν<sub>C=N</sub>, m), 1619 (ν<sub>C=N</sub>, m), 1593 (s), 1578 (m), 1480 (s), 1437 (vs), 1291 (m), 1026 (m), 863 (w), 760 (vs), 717 (vs). Anal. calcd for C<sub>59</sub>H<sub>52</sub>Br<sub>2</sub>N<sub>2</sub>Ni (1007.58): C, 70.33; H, 5.20; N, 2.78. Found: C, 70.28; H, 5.22; N, 2.81.

[1-{2,6-(Ph<sub>2</sub>CH)<sub>2</sub>-4-MeC<sub>6</sub>H<sub>2</sub>N}-2-{2-(C<sub>5</sub>H<sub>9</sub>)-4,6-Me<sub>2</sub>C<sub>6</sub>H<sub>2</sub>N}]C<sub>2</sub>C<sub>10</sub>H<sub>6</sub>]NiBr<sub>2</sub> (**Ni5**). Using a similar procedure and molar ratios to that described for **Ni1** but with **L5** as the ligand, **Ni5** was obtained as a red powder (0.04 g, 20%). IR (KBr; cm<sup>-1</sup>): 3012 (w), 2917 (m), 2351 (m), 1646 (ν<sub>C=N</sub>, m), 1620 (ν<sub>C=N</sub>, m), 1593 (s), 1579 (s), 1484 (s), 1442 (vs), 1287 (m), 1021 (m), 850 (w), 764 (s), 704 (vs). Anal. calcd for C<sub>58</sub>H<sub>50</sub>Br<sub>2</sub>N<sub>2</sub>Ni (993.55): C, 70.12; H, 5.07; N, 2.82. Found: C, 70.21; H, 5.21; N, 2.75.

[1-{2,6-(Ph<sub>2</sub>CH)<sub>2</sub>-4-MeC<sub>6</sub>H<sub>2</sub>N}-2-{2-(C<sub>8</sub>H<sub>15</sub>)-4,6-Me<sub>2</sub>C<sub>6</sub>H<sub>2</sub>N}]C<sub>2</sub>C<sub>10</sub>H<sub>6</sub>]NiBr<sub>2</sub> (**Ni6**). Using a similar procedure and molar ratios to that described for **Ni1** but with **L6** as the ligand, **Ni6** was obtained as a red powder (0.16 g, 80%). IR (KBr; cm<sup>-1</sup>): 3025 (w), 2917 (m), 2852 (w), 1647 (ν<sub>C=N</sub>, m), 1623 (ν<sub>C=N</sub>, m), 1579 (s), 1497 (s), 1443 (vs), 1288 (m), 1036 (m), 861 (w), 828 (w), 770 (s), 743 (vs). Anal. calcd for C<sub>61</sub>H<sub>56</sub>Br<sub>2</sub>N<sub>2</sub>Ni (1035.63): C, 70.75; H, 5.45; N, 2.71. Found: C, 70.82; H, 5.39; N, 2.65.

### X-ray crystallographic studies

Single crystals of **Ni1**, **Ni2**, **Ni3** and **Ni5** suitable for the X-ray diffraction analysis were obtained by laying diethyl ether on a dichloromethane solution of the corresponding complex at room temperature. With graphite monochromated Mo-Kα radi-

Table 6 Crystal data and structure refinements for **Ni1**, **Ni2**, **Ni3** and **Ni5**

	<b>Ni1</b>	<b>Ni2</b>	<b>Ni3</b>	<b>Ni5</b>
Empirical formula	C <sub>58</sub> H <sub>50</sub> Br <sub>2</sub> N <sub>2</sub> Ni	C <sub>61</sub> H <sub>58</sub> Br <sub>2</sub> N <sub>2</sub> NiO	C <sub>60</sub> H <sub>54</sub> Br <sub>2</sub> N <sub>2</sub> Ni	C <sub>62</sub> H <sub>60</sub> Br <sub>2</sub> N <sub>2</sub> NiO
Formula weight	993.53	1053.58	1036.64	1067.61
Temperature/K	173.15	173.15	293(2)	293(2)
Wavelength/Å	0.71073	0.71073	0.71073	0.71073
Crystal system	Monoclinic	Monoclinic	Triclinic	Monoclinic
Space group	<i>P2<sub>1</sub>/n</i>	<i>P2<sub>1</sub>/n</i>	<i>P1</i>	<i>P2<sub>1</sub>/c</i>
<i>a</i> /Å	10.658(2)	10.612(2)	10.987(2)	10.526(2)
<i>b</i> /Å	18.896(4)	18.490(4)	12.500(3)	17.767(4)
<i>c</i> /Å	25.117(5)	25.591(5)	19.151(4)	27.812(6)
Alpha/°	90.00	90.00	102.42(3)	90.00
Beta/°	95.19(3)	95.00(3)	93.70(3)	94.73(3)
Gamma/°	90.00	90.00	93.95(3)	90.00
Volume/Å <sup>3</sup>	5037.8(17)	5002.4(17)	2553.9(9)	5183.5(18)
<i>Z</i>	4	4	2	4
<i>D</i> <sub>calcd</sub> /(g cm <sup>-3</sup> )	1.310	1.399	1.439	1.368
<i>μ</i> /mm <sup>-1</sup>	2.009	2.029	2.091	1.959
<i>F</i> (000)	2040.0	2176.0	1136.0	2208.0
Crystal size/mm <sup>3</sup>	0.20 × 0.20 × 0.20	0.14 × 0.10 × 0.09	0.32 × 0.31 × 0.12	0.43 × 0.20 × 0.05
<i>θ</i> range/°	2.70–54.94	3.196–54.97	2.18–55.00	2.72–54.98
Limiting indices	–13 ≤ <i>h</i> ≤ 13 –24 ≤ <i>k</i> ≤ 24 –32 ≤ <i>l</i> ≤ 32	–13 ≤ <i>h</i> ≤ 13 –24 ≤ <i>k</i> ≤ 24 –33 ≤ <i>l</i> ≤ 33	–14 ≤ <i>h</i> ≤ 14 –16 ≤ <i>k</i> ≤ 16 –24 ≤ <i>l</i> ≤ 24	–13 ≤ <i>h</i> ≤ 13 –23 ≤ <i>k</i> ≤ 23 –36 ≤ <i>l</i> ≤ 36
No. of rflns collected	56 893	68 422	28 595	70 411
No. unique rflns	11 483	11 424	11 649	11 865
<i>R</i> (int)	0.0483	0.0415	0.0395	0.0536
No. of params	570	608	643	618
Completeness to <i>θ</i>	99.6%	99.7%	99.1%	99.8%
Goodness of fit on <i>F</i> <sup>2</sup>	1.130	1.107	1.070	1.221
Final <i>R</i> indices [ <i>I</i> ≥ 2σ( <i>I</i> )]	<i>R</i> <sub>1</sub> = 0.0492 <i>wR</i> <sub>2</sub> = 0.1079	<i>R</i> <sub>1</sub> = 0.0486 <i>wR</i> <sub>2</sub> = 0.1225	<i>R</i> <sub>1</sub> = 0.0439 <i>wR</i> <sub>2</sub> = 0.1044	<i>R</i> <sub>1</sub> = 0.0557 <i>wR</i> <sub>2</sub> = 0.1257
<i>R</i> indices (all data)	<i>R</i> <sub>1</sub> = 0.0545 <i>wR</i> <sub>2</sub> = 0.1108	<i>R</i> <sub>1</sub> = 0.0518 <i>wR</i> <sub>2</sub> = 0.1249	<i>R</i> <sub>1</sub> = 0.0488 <i>wR</i> <sub>2</sub> = 0.1077	<i>R</i> <sub>1</sub> = 0.0597 <i>wR</i> <sub>2</sub> = 0.1312
Largest diff. peak and hole/(e Å <sup>-3</sup> )	0.38 and –0.55	0.99 and –1.04	0.72 and –0.65	0.39 and –0.71

ation ( $\lambda = 0.71073 \text{ \AA}$ ) at 173(2) K, cell parameters were obtained by global refinement of the positions of all collected reflections. Intensities were corrected for Lorentz and polarization effects and empirical absorption. The structures were solved by direct methods and refined by full-matrix least squares on  $F^2$ . All hydrogen atoms were placed in calculated positions. Structure solution and refinement were performed by using the Olex2 1.2 package.<sup>25</sup> Details of the X-ray structure determinations and refinements are provided in Table 6.

### Polymerization studies

**Ethylene polymerization at 1 atm ethylene pressure.** The polymerization at 1 atm ethylene pressure was carried out in a Schlenk tube. Complex Ni6 was added followed by toluene (30 mL) and then the required amount of co-catalyst (EASC, MMAO) introduced by syringe. The solution was then stirred at 30 °C under 1 atm of ethylene pressure. After 30 min, the solution was quenched with 10% hydrochloric acid in ethanol. The polymer was washed with ethanol, dried under reduced pressure at 40 °C and then weighed.

**Ethylene polymerization at 5/10 atm ethylene pressure.** The polymerization at high ethylene pressure was carried out in a stainless-steel autoclave (0.25 L) equipped with an ethylene pressure control system, a mechanical stirrer and a temperature controller. At the required reaction temperature, the pre-catalyst (2.0  $\mu\text{mol}$ ) dissolved in toluene (50 mL) was injected into the autoclave, followed by freshly distilled toluene (25 mL). The required amount of co-catalyst (MAO, MMAO,  $\text{Et}_2\text{AlCl}$ , EASC) and more toluene (25 mL) were then injected successively to complete the addition. The autoclave was immediately pressurized to high ethylene pressure and the stirring commenced. After the required reaction time, the ethylene pressure was vented and the reaction quenched with 10% hydrochloric acid in ethanol. The polymer was collected and washed with ethanol and dried under reduced pressure at 50 °C and weighed.

### Conflicts of interest

There are no conflicts to declare.

### Acknowledgements

This work was supported by the National Natural Science Foundation of China (No. 21374123 and U1362204) and the National Key Research and Development Program of China (2016YFB1100800). GAS thanks the Chinese Academy of Sciences for a Visiting Professorship.

### References

- (a) L. K. Johnson, C. M. Killian and M. Brookhart, *J. Am. Chem. Soc.*, 1995, **117**, 6414; (b) L. K. Johnson, S. Mecking and M. Brookhart, *J. Am. Chem. Soc.*, 1996, **118**, 267.
- (a) G. J. P. Britovsek, V. C. Gibson, S. J. McTavish, G. A. Solan, A. J. P. White, B. S. Kimberley, P. J. Maddox and D. J. Williams, *Chem. Commun.*, 1998, 849; (b) G. J. P. Britovsek, M. Bruce, V. C. Gibson, B. S. Kimberley, P. J. Maddox, S. Mastroianni, S. J. McTavish, C. Redshaw, G. A. Solan, S. Strömberg, A. J. P. White and D. J. Williams, *J. Am. Chem. Soc.*, 1999, **121**, 8728.
- (a) L. Zhong, G. Li, G. Liang, H. Gao and Q. Wu, *Macromolecules*, 2017, **50**, 2675; (b) Z. Wang, Q. Liu, G. A. Solan and W.-H. Sun, *Coord. Chem. Rev.*, 2017, DOI: 10.1016/j.ccr.2017.06.003; (c) Z. Wang, Y. Zhang, Y. Ma, X. Hu, G. A. Solan, Y. Sun and W.-H. Sun, *J. Polym. Sci., Part A: Polym. Chem.*, 2017, **55**, 3494–3505.
- (a) M. Helldörfer, J. Backhaus, W. Milius and H. G. Alt, *J. Mol. Catal. A: Chem.*, 2003, **193**, 59; (b) M. Helldörfer, J. Backhaus and H. G. Alt, *Inorg. Chim. Acta*, 2003, **351**, 34; (c) D. H. Camacho and Z. Guan, *Chem. Commun.*, 2010, **46**, 7879; (d) D. P. Gates, S. A. Svejda, E. Oñate, C. M. Killian, L. K. Johnson, P. S. White and M. Brookhart, *Macromolecules*, 2000, **33**, 2320; (e) F. Alobaidi, Z. Ye and S. Zhu, *Polymer*, 2004, **45**, 6823; (f) F.-S. Liu, H.-B. Hu, Y. Xu, L.-H. Guo, S.-B. Zai, K.-M. Song, H.-Y. Gao, L. Zhang, F.-M. Zhu and Q. Wu, *Macromolecules*, 2009, **42**, 7789; (g) D. Meinhard, M. Wegner, G. Kipiani, A. Hearley, P. Reuter, S. Fischer, O. Marti and B. Rieger, *J. Am. Chem. Soc.*, 2007, **129**, 9182; (h) S. D. Ittel, L. K. Johnson and M. Brookhart, *Chem. Rev.*, 2000, **100**, 1169; (i) C. Bianchini, G. Giambastiani, L. Luconi and A. Meli, *Coord. Chem. Rev.*, 2010, **254**, 431; (j) G. J. P. Britovsek, S. P. D. Baugh, O. Hoarau, V. C. Gibson, D. F. Wass, A. J. P. White and D. J. Williams, *Inorg. Chim. Acta*, 2003, **345**, 279; (k) W.-H. Sun, S. Jie, S. Zhang, W. Zhang, Y. Song and H. Ma, *Organometallics*, 2006, **25**, 666.
- (a) J. L. Rhinehart, N. E. Mitchell and B. K. Long, *ACS Catal.*, 2014, **4**, 2501; (b) J. L. Rhinehart, L. A. Brown and B. K. Long, *J. Am. Chem. Soc.*, 2013, **135**, 16316.
- D. Zhang, E. T. Nadres, M. Brookhart and O. Daugulis, *Organometallics*, 2013, **32**, 5136.
- (a) H. Liu, W. Zhao, X. Hao, C. Redshaw, W. Huang and W.-H. Sun, *Organometallics*, 2011, **30**, 2418; (b) S. Kong, C. Guo, W. Yang, L. Wang, W.-H. Sun and R. Glaser, *J. Organomet. Chem.*, 2013, **725**, 37; (c) L. Fan, S. Du, C. Guo, X. Hao and W.-H. Sun, *J. Polym. Sci., Part A: Polym. Chem.*, 2015, **53**, 1369; (d) W. Zhao, E. Yue, X. Wang, W. Yang, Y. Chen, X. Hao, X. Cao and W.-H. Sun, *J. Polym. Sci., Part A: Polym. Chem.*, 2017, **55**, 988.
- (a) Z. Sun, E. Yue, M. Qu, I. V. Oleynik, I. I. Oleynik, K. Li, T. Liang, W. Zhang and W.-H. Sun, *Inorg. Chem. Front.*, 2015, **2**, 223; (b) Z. Sun, F. Huang, M. Qu, E. Yue, I. V. Oleynik, I. I. Oleynik, Y. Zeng, T. Liang, K. Li, W. Zhang and W.-H. Sun, *RSC Adv.*, 2015, **5**, 77913; (c) S. S. Ivanchev, G. A. Tolstikov, V. K. Badaev, I. I. Oleinik, N. I. Ivancheva, D. G. Rogozin, I. V. Oleinik and S. V. Myakin, *Kinet. Catal.*, 2004, **45**, 176; (d) S. S. Ivanchev, G. A. Tolstikov, V. K. Badaev, N. I. Ivancheva, I. I. Oleinik,

- S. Y. Khaikin and I. V. Oleinik, *Polym. Sci., Ser. A*, 2002, **44**, 931; (e) S. S. Ivanchev, G. A. Tolstikov, V. K. Badaev, N. I. Ivancheva, I. I. Oleinik, M. I. Serushkin and L. V. Oleinik, *Polym. Sci., Ser. A*, 2001, **43**, 1189; (f) I. I. Oleinik, I. V. Oleinik, I. B. Abdrakhmanov, S. S. Ivanchev and G. A. Tolstikov, *Russ. J. Gen. Chem.*, 2004, **74**, 1575; (g) I. I. Oleinik, I. V. Oleinik, I. B. Abdrakhmanov, S. S. Ivanchev and G. A. Tolstikov, *Russ. J. Gen. Chem.*, 2004, **74**, 1423; (h) I. I. Oleinik, I. V. Oleinik, S. S. Ivanchev and G. A. Tolstikov, *Russ. J. Org. Chem.*, 2005, **41**, 1329; (i) G. S. Zhilovskii, I. I. Oleinik, S. S. Ivanchev and G. A. Tolstikov, *Russ. J. Org. Chem.*, 2009, **45**, 44.
- 9 (a) C. Lee, S. P. Gido, Y. Poulos, N. Hadjichristidis, N. B. Tan, S. F. Trevino and J. W. Mays, *J. Chem. Phys.*, 1997, **107**, 6460; (b) W. A. Braunecker and K. Matyjaszewski, *Prog. Polym. Sci.*, 2007, **32**, 93.
- 10 M. Akiba and A. S. Hashim, *Prog. Polym. Sci.*, 1997, **22**, 475.
- 11 B. Adhikari, D. De and S. Maiti, *Prog. Polym. Sci.*, 2000, **25**, 909.
- 12 (a) X. Wang, L. Fan, Y. Ma, C. Guo, G. A. Solan, Y. Sun and W.-H. Sun, *Polym. Chem.*, 2017, **8**, 2785; (b) H. Liu, W. Zhao, J. Yu, W. Yang, X. Hao, C. Redshaw, L. Chen and W.-H. Sun, *Catal. Sci. Technol.*, 2012, **2**, 415; (c) Q. Mahmood, Y. Zeng, E. Yue, G. A. Solan, T. Liang and W.-H. Sun, *Polym. Chem.*, 2017, DOI: 10.1039/C7PY01606A.
- 13 L. Zhu, D. Zang, Y. Wang, Y. Guo, B. Jiang, F. He, Z. Fu, Z. Fan, M. A. Hickner, Z.-K. Liu and L.-Q. Chen, *Organometallics*, 2017, **36**, 1196.
- 14 E. Y.-X. Chen and T. J. Marks, *Chem. Rev.*, 2000, **100**, 1391.
- 15 S. Du, S. Kong, Q. Shi, J. Mao, C. Guo, J. Yi, T. Liang and W.-H. Sun, *Organometallics*, 2015, **34**, 582.
- 16 (a) S. Du, Q. Xing, Z. Flisak, E. Yue, Y. Sun and W.-H. Sun, *Dalton Trans.*, 2015, **44**, 12282; (b) X. Wang, L. Fan, Y. Yuan, S. Du, Y. Sun, G. A. Solan, C. Y. Guo and W.-H. Sun, *Dalton Trans.*, 2016, **45**, 18313; (c) Q. Mahmood, Y. Zeng, X. Wang, Y. Sun and W.-H. Sun, *Dalton Trans.*, 2017, **46**, 6934; (d) L. Fan, E. Yue, S. Du, C. Guo, X. Hao and W.-H. Sun, *RSC Adv.*, 2015, **5**, 93274.
- 17 H. Gao, H. Hu, F. Zhu and Q. Wu, *Chem. Commun.*, 2012, **48**, 3312.
- 18 (a) G. Leone, M. Mauri, I. Pierro, G. Ricci, M. Canetti and F. Bertini, *Polymer*, 2016, **100**, 37; (b) G. B. Galland, R. F. Souza, R. S. Mauler and F. F. Nunes, *Macromolecules*, 1999, **32**, 1620.
- 19 B. Gabrielle, L. Guy, P.-A. Albouy, L. Vanel, D. R. Long and P. Sotta, *Macromolecules*, 2011, **44**, 7006.
- 20 Y. Kong and J. N. Hay, *Polymer*, 2002, **43**, 3873.
- 21 (a) G. R. Hamed and N. R. Attanasom, *Rubber Chem. Technol.*, 2002, **75**, 935; (b) B. Gabrielle, L. Guy, P. A. Albouy, L. D. Vanel, R. Long and P. Sotta, *Macromolecules*, 2011, **44**, 7006; (c) W. Wiyatno, G. G. Fuller, J. A. Pople, A. P. Gast, Z. Chen, R. M. Waymouth and C. L. Myers, *Macromolecules*, 2003, **36**, 1178; (d) S. Li, F. Wu, Y. Wang and J. Zeng, *Ind. Eng. Chem. Res.*, 2015, **54**, 6258.
- 22 J. R. Martin, J. F. Johnson and A. R. Cooper, *J. Macromol. Sci., Part C*, 1972, **8**, 57.
- 23 Z. He, Y. Liang, W. Yang, H. Uchino, J. Yu, W.-H. Sun and C. C. Han, *Polymer*, 2015, **56**, 119.
- 24 S. Li, J. Zeng, F. Wu, Y. Yang and Y. Wang, *Ind. Eng. Chem. Res.*, 2014, **53**, 1404.
- 25 O. V. Dolomanov, L. J. Bourhis, R. J. Gildea, J. A. K. Howard and H. Puschmann, *J. Appl. Crystallogr.*, 2009, **42**, 339.